YMTHE, Volume *30*

Supplemental Information

mRNA-LNP vaccines tuned for systemic immunization induce strong antitumor immunity by engaging splenic immune cells

Sanne Bevers, Sander A.A. Kooijmans, Elien Van de Velde, Martijn J.W. Evers, Sofie Seghers, Jerney J.J.M. Gitz-Francois, Nicky C.H. van Kronenburg, Marcel H.A.M. Fens, Enrico Mastrobattista, Lucie Hassler, Helena Sork, Taavi Lehto, Kariem E. Ahmed, Samir El Andaloussi, Katja Fiedler, Karine Breckpot, Michael Maes, Diane Van Hoorick, Thierry Bastogne, Raymond M. Schiffelers, and Stefaan De Koker

Supplementary method: Bayesian-based Quality by Design

A Bayesian implementation of the Quality by Design (QbD) good development practice (ICH Q8(R2))[1] was applied for the lipid based nanoparticle (LNP) optimization. The Bayesian inference is often qualified as more natural than the conventional frequentist statistics in the sense that science works namely the same way. In a scientific approach, today's prior is updated by new data to become a posterior distribution that will serve as tomorrow's prior, and so forth. The same applies to the Quality by Design cycle (Fig. 1) based on a deductive/inductive reasoning process. Any QbD cycle relies on an investigation model describing the cause-effect relationship between input factors (CMA: critical material attributes and CPP: critical process parameters) and output responses (CQA: critical quality attributes). The last three steps of the QbD cycle (experimentation, empirical modeling and knowledge) are detailed below. The Bayesian implementation of the empirical modeling was performed within the R statistical computing environment[2].

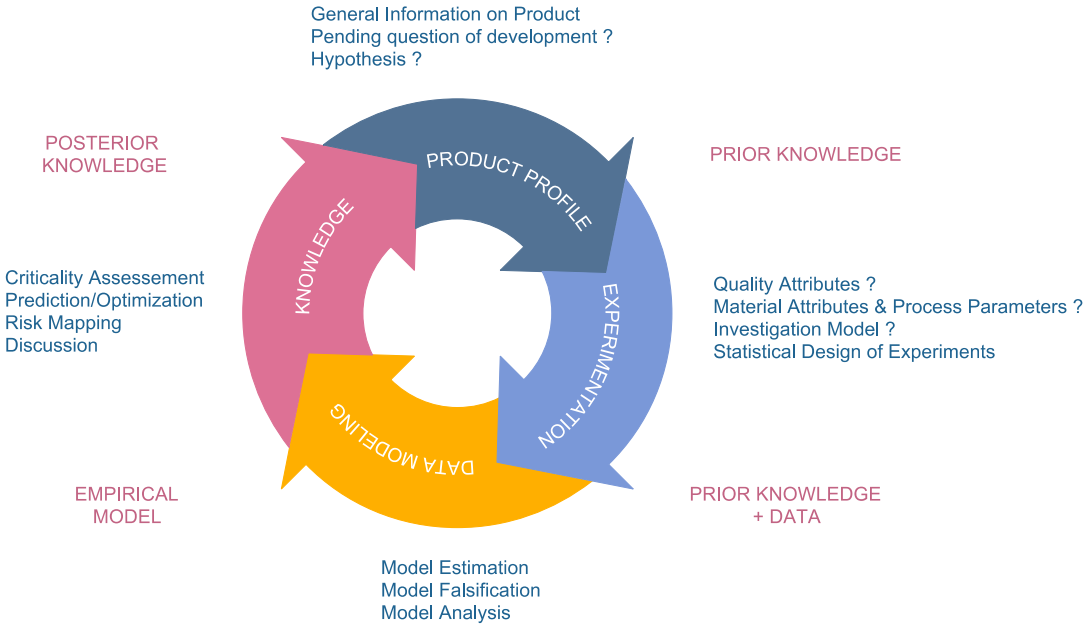

Figure 1: Quality by Design approach presented as a deductive/inductive reasoning process in which Bayesian statistics are introduced to estimate and assess models of investigation, but also to predict quality attributes (response variables) and risks to not meet expected specifications on CQA.

Pending Question & Quality Attribute

In this study we aimed to optimize the formulation of mRNA-lipid nanoparticles in order to achieve the maximal possible immune response. Accordingly, the critical quality attribute to be controlled is the CD8 T cell response, determined as %E7-specific T cells in blood of mice after three immunizations. The expected specification is to meet the minimum level of 50%.

Critical Material Attributes

Three constitutive lipid proportions were considered as three independent critical material attributes (CMA). The range of each lipid proportion was selected based on prior knowledge and is summarized in Table 1. Cholesterol (u4) constitutes the remainder of the lipid mix (fill molar proportion up to 100%).

Notation	Critical material attributes	Experimental domain (molar lipid proportion in %)
u1	Ionizable lipid	35 - 65
u2	PEG-lipid	0.5 - 2
u3	DOPE	5 - 15

Table 1: Critical material attributes and their respective experimental domain.

Design of Experiments

A Roquemore's Hybrid Design was used to select the formulations to be tested (i.e. the trials to be carried out). Each experimental condition was applied in triplicate (3 mice/treatment). Each lipid's molar percentage takes five values, and the design is composed of 11 different experimental conditions (Table 2). This experimental protocol was carried out for three different choices of PEG-lipid. This design is particularly suited to the identification of quadratic response surface models (see next section) and more economic than a central composite design (15 assays) or Box-Behnken design (13 assays).

N°Exp	IonizLipid	PEGLipid	DOPE
	%	%	%
1	50	1.25	15
2	50	1.25	5
3	40.5	0.78	12.24
4	59.5	0.78	12.24
5	40.5	1.72	12.24
6	59.5	1.72	12.24
7	36.6	1.25	7.76
8	63.4	1.25	7.76
9	50	0.58	7.76
10	50	1.92	7.76
11	50	1.25	10

Table 2: Roquemore's Hybrid Design of Experiments

Investigation Model

The investigation model used to optimize the LNP composition is described by a quadratic response surface model structure:

$$Y_k = b_0 + \sum_{i=1}^{3} b_i \, u_{i,k} + \sum_{i=1}^{3} b_{ii} \, u_{i,k}^2 + \sum_{i=1}^{2} \sum_{j=2}^{3} b_{ij} \, u_{i,k} \, u_{j,k} + E_k$$

with:

- k=1,⋯,n: is the index of the experimental condition in the experimental design ;
- n: is the total number of experiments to be carried out;
- Y_k: value of %E7-specific T cells in blood for the k-th assay of the design;
- b_0: value of the mean response;
- b_i: additive effect of the i-th factor;
- b_{ii}: quadratic effect of the i-th factor;
- b_{ij}: interaction effect between the i-th and j-th factors on the response;
- $E_k \sim N(0,\sigma 2)$: random error describing modeling residual.

All the model coefficients b_i, b_{ii} and b_{ij} have to be estimated from the experimental data collected after experimentation.

Bayesian estimation of the model parameters

After obtaining data on the T-cell stimulatory capacity (%E7-specific CD8 T cells) of the LNP formulations in mice, the data was used to construct a quadratic response surface model. The Hamiltonian Monte Carlo (HMC) algorithm, a generalization of the Metropolis algorithm[3], was used to compute the posterior distributions of the model parameters. Simulations from the HMC are determined by Bayes' rule, in which the posterior distribution of the parameters is proportional to the prior distribution of the parameters multiplied by the likelihood. Main percentile values characterizing dispersion and uncertainty of the model parameters are given in Table 3 (and interpreted in section "Tests of significance and criticality")

A

	mean	sd	25%	50%	75%
(Intercept)	113.08	76.53	62.61	113.02	162.87
u1	0.65	2.04	-0.67	0.63	1.95
u2	-137.65	39.89	-164.07	-137.60	-111.73
u3	-4.14	5.22	-7.48	-4.15	-0.81
I(u1^2)	0.00	0.02	-0.01	0.00	0.02
I(u2^2)	29.73	10.53	22.92	29.76	36.79
I(u3^2)	0.13	0.20	0.00	0.13	0.26
u1:u2	-0.03	0.52	-0.38	-0.03	0.32
u1:u3	-0.08	0.07	-0.13	-0.08	-0.03
u2:u3	3.79	1.62	2.73	3.83	4.86
sigma	8.56	1.32	7.61	8.40	9.34

B

	mean	sd	25%	50%	75%
(Intercept)	11.53	90.95	-47.29	13.29	72.37
u1	2.58	2.47	0.99	2.45	4.18
u2	-52.95	44.04	-81.36	-52.61	-24.63
u3	-6.19	6.42	-10.50	-6.07	-1.84
I(u1^2)	-0.01	0.02	-0.02	-0.01	0.01
I(u2^2)	29.61	11.63	22.06	29.66	37.39
I(u3^2)	-0.31	0.24	-0.46	-0.31	-0.15
u1:u2	-1.89	0.63	-2.32	-1.90	-1.47
u1:u3	0.12	0.09	0.06	0.12	0.18
u2:u3	4.83	1.84	3.62	4.86	6.06
sigma	10.06	1.53	9.00	9.88	10.96

C

	mean	sd	25%	50%	75%
(Intercept)	-167.89	135.06	-260.62	-161.43	-71.64
u1	6.80	3.96	3.92	6.57	9.52
u2	-15.39	49.51	-47.11	-13.98	16.03
u3	6.65	7.80	1.40	6.53	11.91
I(u1^2)	-0.06	0.04	-0.08	-0.05	-0.03
I(u2^2)	-17.33	14.27	-26.91	-17.15	-7.90
I(u3^2)	-0.58	0.31	-0.79	-0.57	-0.37
u1:u2	-0.06	0.69	-0.50	-0.06	0.39
u1:u3	0.00	0.10	-0.06	0.00	0.07
u2:u3	4.14	2.26	2.62	4.14	5.59
sigma	12.51	1.95	11.11	12.30	13.71

Table 3: Mean, standard deviation and main percentile values characterizing dispersion and uncertainty of the model parameters. A: DMG-PEG2000 model; B: DSG-PEG2000 model and C: DSPE-PEG1000 model.

Posterior predictive check

The posterior predictive check (PPC)[4] is a Bayesian technique to assess the appropriateness of the model to fit data.[3] A “good” model is able to simulate data close to the observations as illustrated in Figure 2.

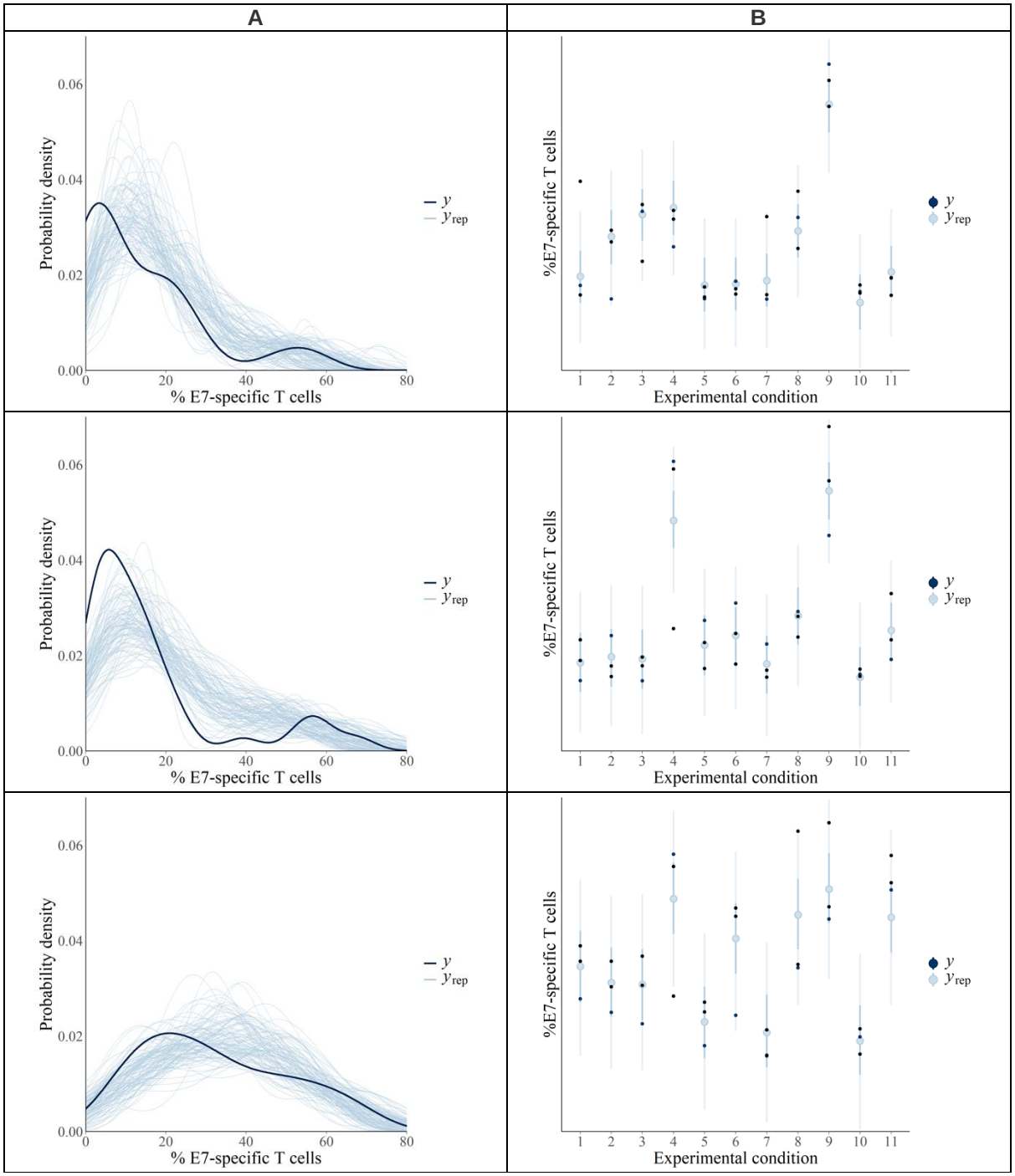

Figure 2: A) Observed vs replicated data densities for E7-specific T cell response. The density line in dark blue indicates the smooth density of observed data compared to overlaid smooth densities of 100 replicated data in light blue. B) Points in dark indicate observations of the 11 conditions tested in triplicate. Each line in light blue represents the posterior predictive distribution for each condition. Top to bottom DMG-PEG2000 model, DSG-PEG2000 model and DSPE-PEG1000 model.

To summarize data fitting performance a Bayesian version of the coefficient of determination (R^2) was computed. This coefficient uses draws from the residual distribution and is defined as the variance of the predicted values divided by the variance of the predicted values plus the variance of residuals (differences between fitted values and observed data)[5]. Figure 3 shows Bayesian R^2 mean values larger for DMG-PEG2000 and DSG-PEG2000 (≈0.72) than DPSE-PEG1000 (≈0.59).

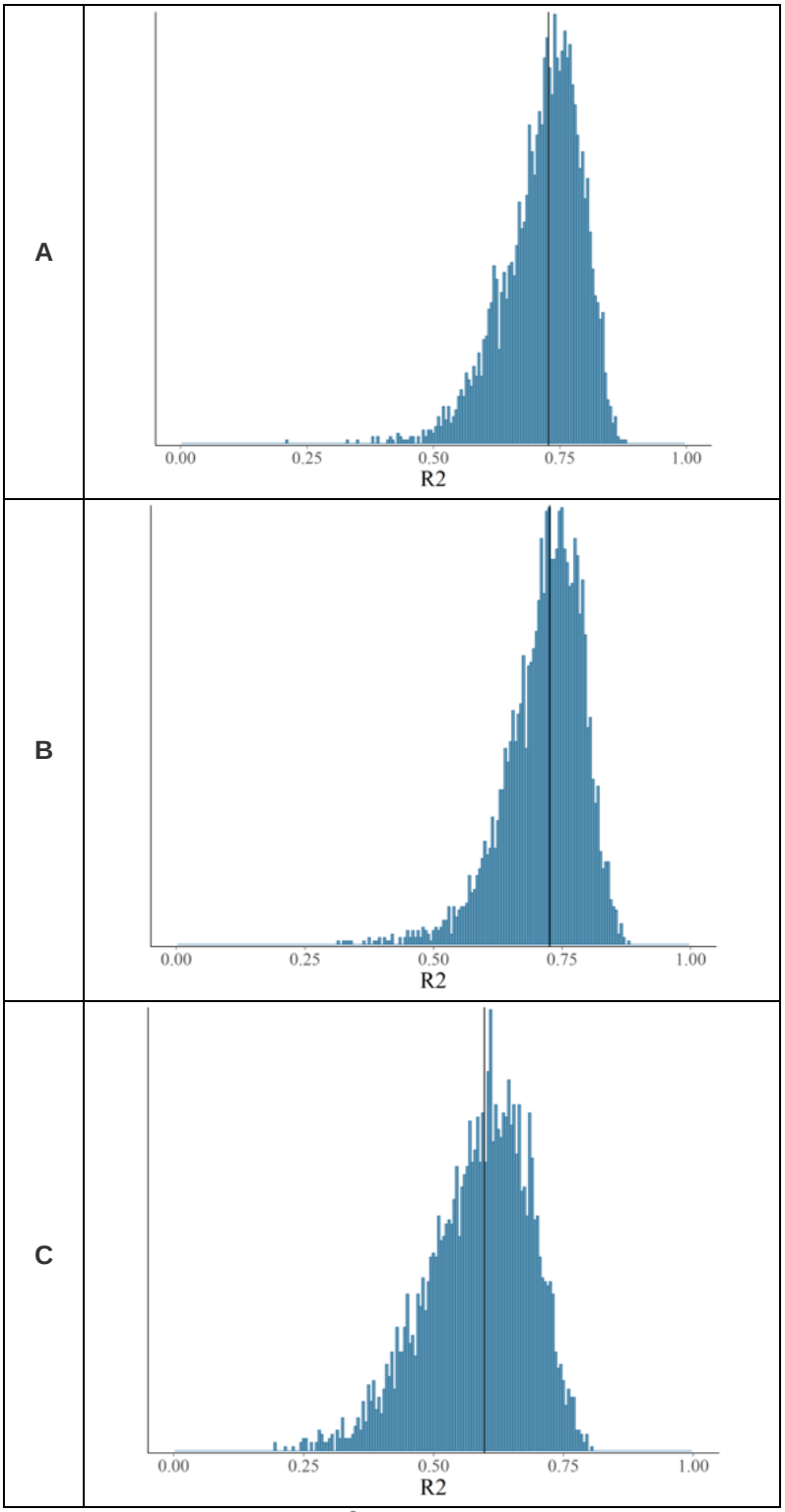

Figure 3: Histogram of the Bayesian version of the R^2 coefficient of determination computed over 4000 replicated data of CD8 T cell response. A: DMG-PEG2000 model; B: DSG-PEG2000 model and C: DSPE-PEG1000 model.

Analysis of posterior distributions related to the model parameters

Tests of significance and criticality

Effect analysis is often implemented as statistical tests applied to each model parameter, in which p-values play a key role. Nevertheless, several controversialities have recently emerged about their use and interpretation[6–8]. The way that p-values have been informally defined and interpreted appears to have led to tremendous confusion and controversy regarding their place in statistical analysis. To avoid those trick questions, posterior distributions of model parameters were directly used to estimate their criticality. The *modus operandi* implemented to analyze effects of each factor (i.e. lipid component of the LNPs) is described in Figure 4. Each subfigure is composed of a posterior distribution of a model parameter b (see investigation model) describing either single, quadratic or interaction effects. Two different aspects have to be examined: significance and criticality of effects.

- Significance of the effect (test of nullity): Examining the position of the distribution with respect to the origin of the X-axis:
  $$\begin{cases} H0s: & b = 0 \\ H1s: & b \neq 0 \end{cases} \quad (1)$$
  We used the equation $p_s = P[H0s]$. If $p_s < \pi_s$, significance of the effect b is accepted. π_s is a threshold probability of significance.
- Criticality of the effect is assessed by examining the position of the same distribution with respect to a threshold d: the smallest mean value of the effect considered as critical.
  $$\begin{cases} H0c: & |b| > d \\ H1c: & |b| \not> d \end{cases} \quad (2)$$
  We used the equation $p_c = P[H0c]$. If $p_c > \pi_c$, criticality of the effect b is accepted. π_c is a threshold probability of criticality.

Six situations can occur and are illustrated in Figure 4. In cases 1 and 4, posterior distributions are beyond the threshold d, showing critical effects even if uncertainty on the effect magnitude is greater in case 4. On the contrary, cases 2 and 3 do not show any critical effects. The trickiest situation is presented in cases 5 and 6, where two contradictory conclusions may be drawn. In those both risky cases, the effect b is classified “at-risk” until more informative data is collected to definitively conclude.

According to the type of effect (simple, interaction of quadratic) different threshold values can be chosen. In this application, d was fixed to 5, i.e., a variation of 5% of the E7-specific T cell response caused by a 1% change in u_i, u_iu_j or u_i^2 respectively. Note that each factor was normalized before the estimation step. After normalization, all factors take values between -1 and +1 associated with minimal and maximal values in their real scale. Consequently, 1% of change for u_i corresponds to 1% of variation in lipid percentage within its experimental domain presented above in Table 1.

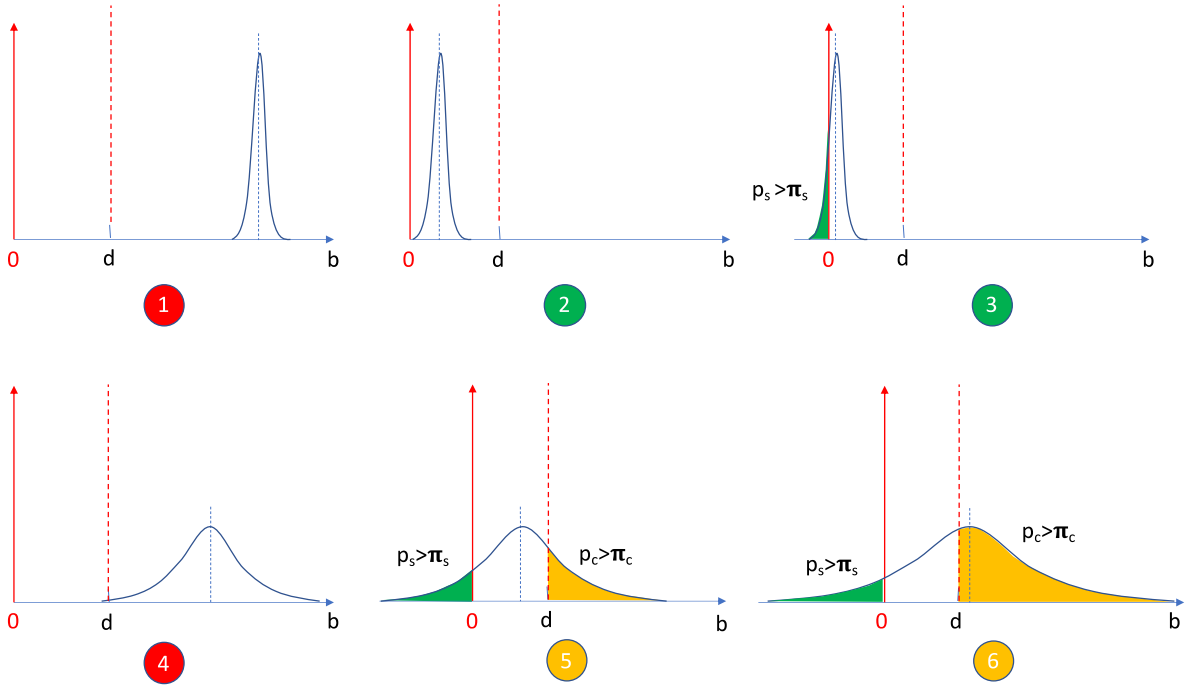

1 - b is both **significant** and **critical**.	2- b is **significant** ($p_s<\pi_s$) but **not critical**.	3 - b is neither **significant** ($p_s>\pi_s$) nor **critical**
4 - b is both **significant** and **critical**.	5 – Uncertain situation: conclusions on **significance** ($p_s>\pi_s$) and **criticality** ($p_c>\pi_c$) are contradictory.	6 - Uncertain situation: conclusions on **significance** ($p_s>\pi_s$) and **criticality** ($p_c>\pi_c$) are contradictory.

b: estimated effect, d: critical effect (threshold)

Figure 4: Schematic showing differences between significance and criticality of effects.

DMG-PEG2000

Figure 5A shows a critical single effect of the %PEG-lipid (u2) and emphasizes a meaningful risk for the %ionizable lipid (u1) and %DOPE (u3) to have a critical impact on the T cell response. Figure 5B points out a critical interaction between %DMG-PEG2000 and %DOPE and potentially between %ionizable lipid and %DOPE. The risk of an interaction between %ionizable lipid and %PEG-lipid impacting the T cell response still exists but is less likely. Figure 5C presents the quadratic effects and confirms the same conclusions drawn for the single effects, i.e. a critical influence of %DMG-PEG2000, and likely impacts of the two other lipids.

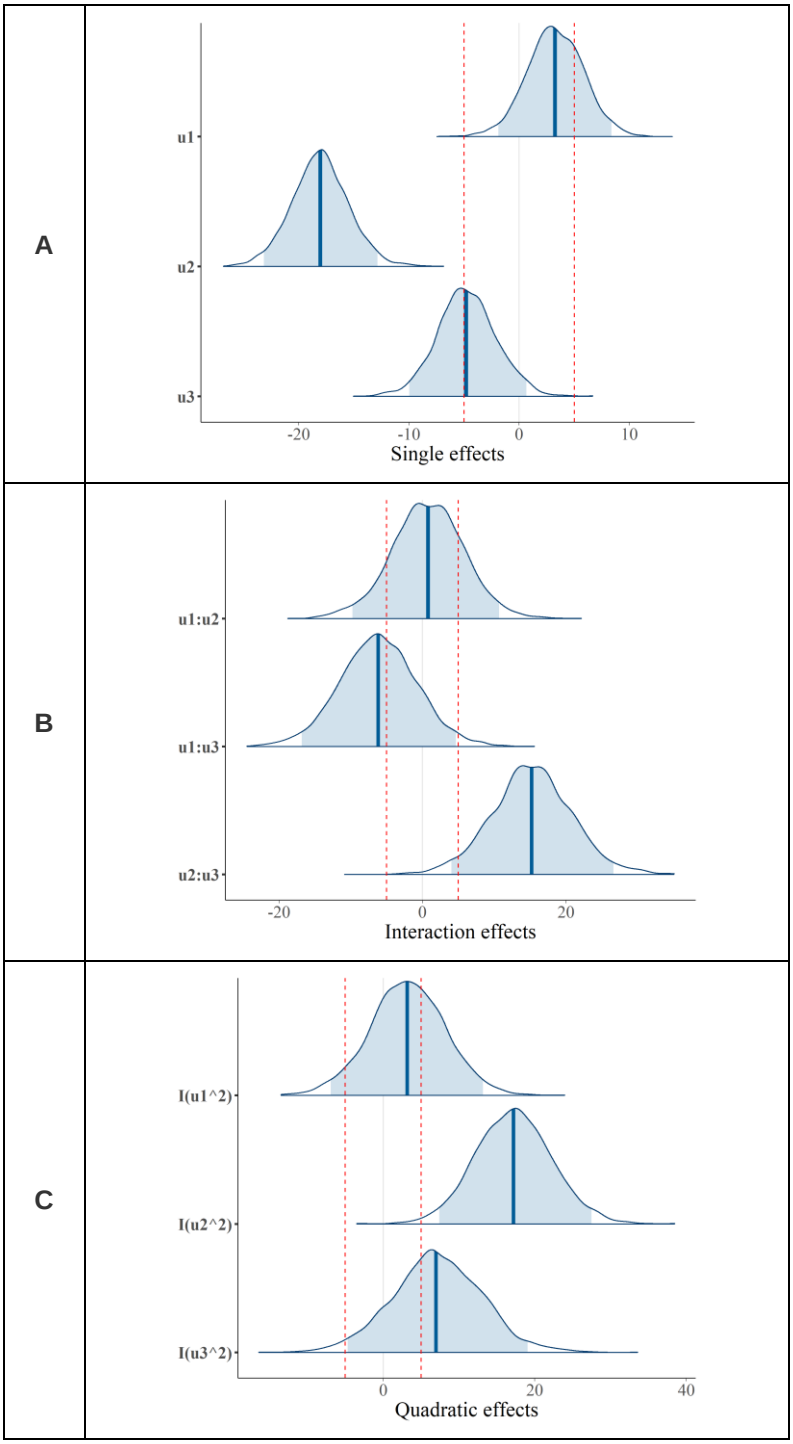

Figure 5: Analysis of individual lipid effects on T cell responses for DMG-PEG2000-based LNPs. Posterior distributions with 95% confidence interval of additive effects for the three studied factors. B: Posterior distributions of interactions effects between factors. C: Posterior distrbutions of quadratic effects. Red dashed lines indicate threshold d to detemine criticality of the effect.

DSG-PEG2000

Figure 6A confirms the critical impact of the %PEG-lipid (u2), already observed for DMG-PEG2000 LNPs (Figure 5a). It concerns both single (Figure 6A) and quadratic effects (Figure 6C) but also interactions with the two other lipid proportions (Figure 6B). Figure 6A also reveals a single effect of %ionizable lipid (u1), which is more critical than estimated for DMG-PEG2000 LNPs (Figure 5a). On the contrary, %DOPE (u3) does not show any critical single effect, but an important interaction with the %PEG-lipid and %ionizable lipid (Figure 6B) and a potential quadratic influence (Figure 6C) on the T cell response.

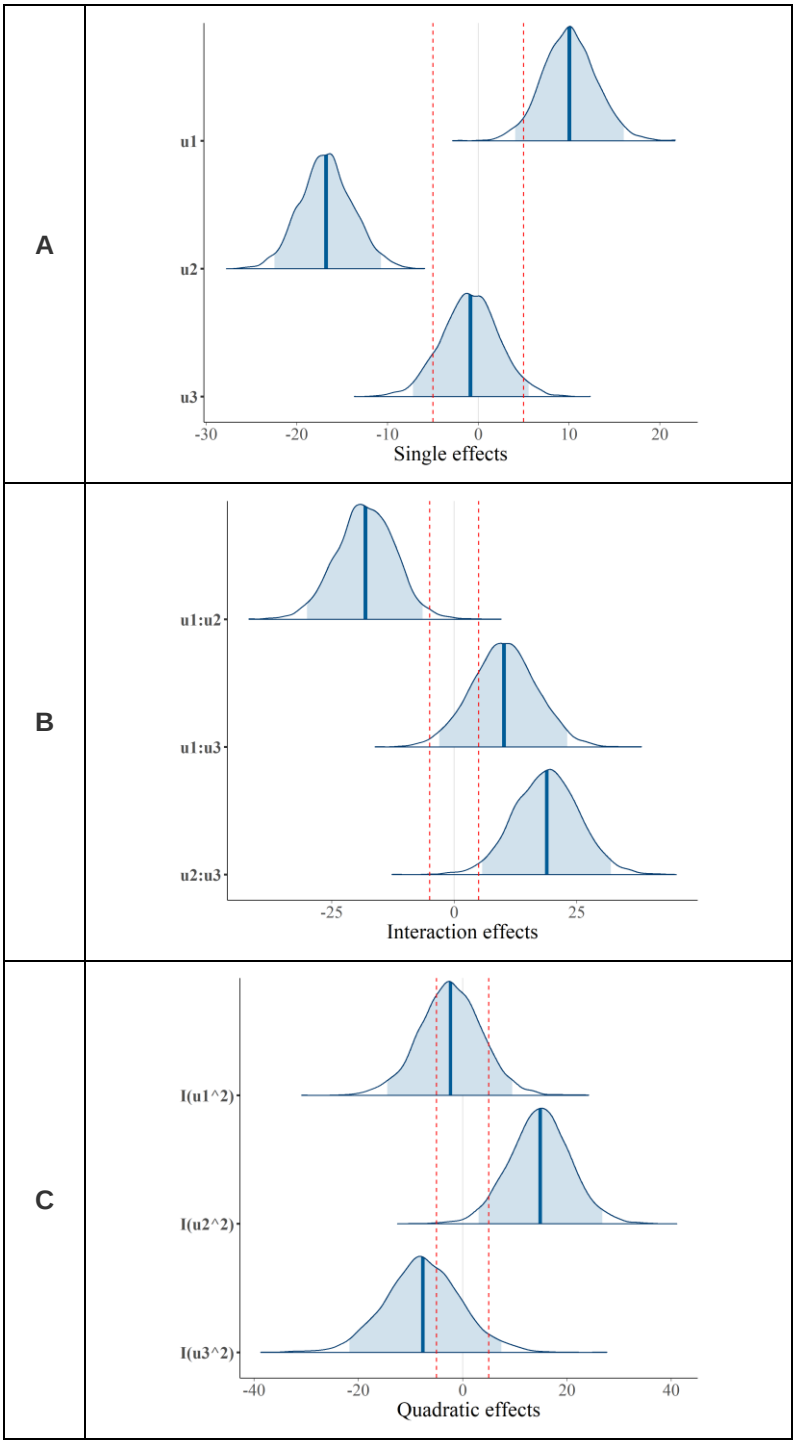

Figure 6: Analysis of individual lipid effects on T cell responses for DSG-PEG2000-based LNPs. Posterior distributions with 95% confidence interval of additive effects for the three studied factors. B: Posterior distributions of interactions effects between factors. C: Posterior distrbutions of quadratic effects. Red dashed lines indicate threshold d to detemine criticality of the effect.

DSPE-PEG1000:

Single effects presented in Figure 7A are very similar to the ones observed in Figure 6A for DSG-PEG2000 LNPs and identify %PEG-lipid (u3) and % ionizable lipid (u1) as critical. Only one interaction seems to be critical and involves %PEG-lipid and %DOPE. On the contrary, all lipid proportions have a critical quadratic influence on the T cell response.

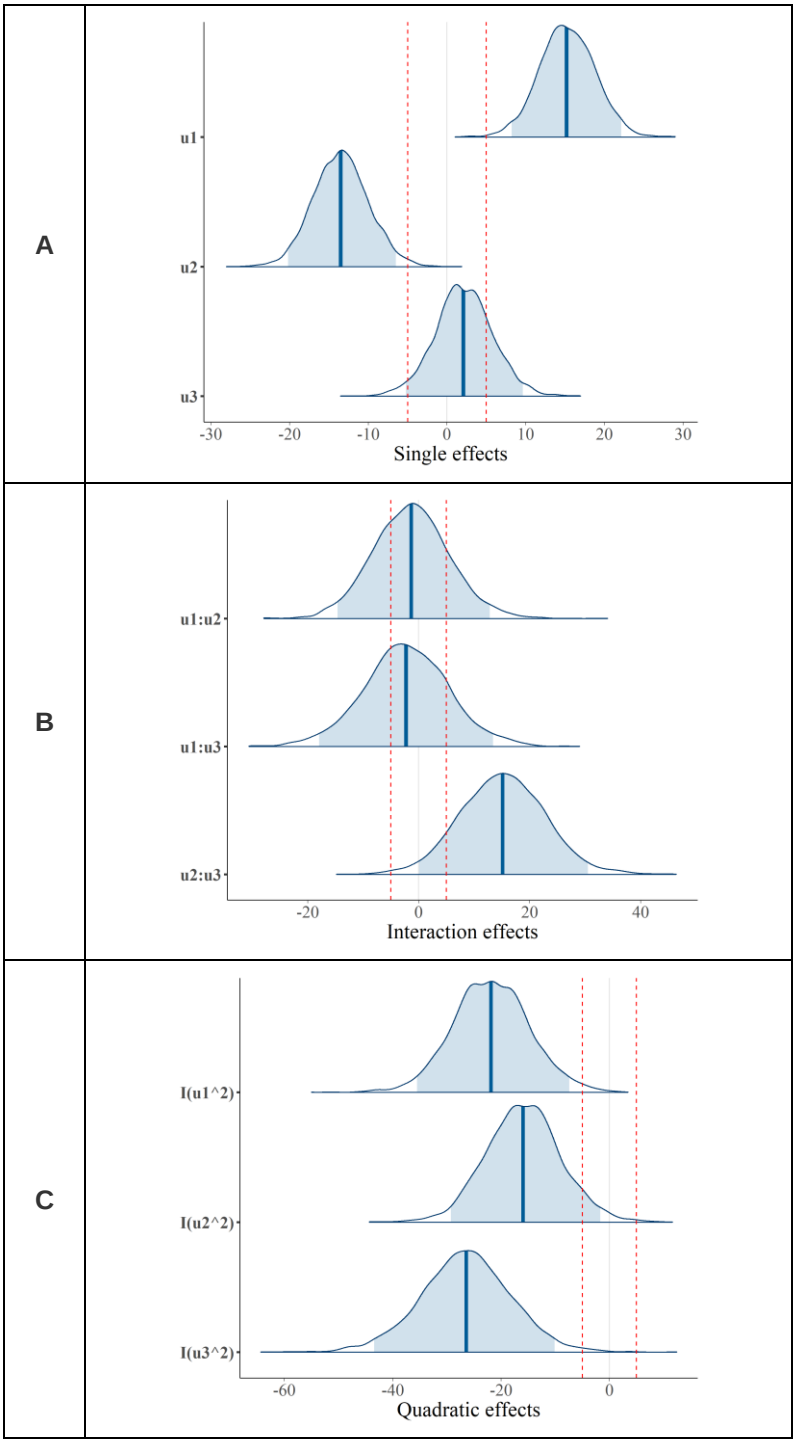

Figure 7: Analysis of individual lipid effects on T cell responses for DSPE-PEG1000 based LNPs. Posterior distributions with 95% confidence interval of additive effects for the three studied factors. B: Posterior distributions of interactions effects between factors. C: Posterior distributions of quadratic effects. Red dashed lines indicate threshold d to detemine criticiality of the effect.

To conclude on the effect analysis, critical effects that are very likely are as follows (listed in order of strength of the effect within the effect type and PEG-lipid type):

- Single effects
    - DMG-PEG2000: PEG-lipid
    - DSG-PEG2000: PEG-lipid and ionizable lipid
    - DSPE-PEG1000: PEG-lipid and ionizable lipid
- Interaction effects
    - DMG-PEG2000: PEG-lipid and DOPE
    - DSG-PEG2000: PEG-lipid and DOPE; ionizable lipid and PEG-lipid; ionizable lipid and DOPE
    - DSPE-PEG1000: PEG-lipid and DOPE
- Quadratic effects
    - DMG-PEG2000: PEG-lipid
    - DSG-PEG2000: PEG-lipid
    - DSPE-PEG1000: DOPE, ionizable lipid, PEG-lipid

To summarize and compare their global effects on the T cell response, results of a global sensitivity analysis are presented in the next section.

Global sensitivity analysis

Single, quadratic and interaction effects can sometimes offset each other. To globally test their impact on the response, a global sensitivity analysis was performed. This global analysis accounts for all types of effect (single, quadratic and interaction). Sensitivity indices of the %E7-specific T cells with respect to the three lipid proportions were computed based on a Monte Carlo estimation of the Sobol' indices[9]. Results are shown in Figure 8.

A

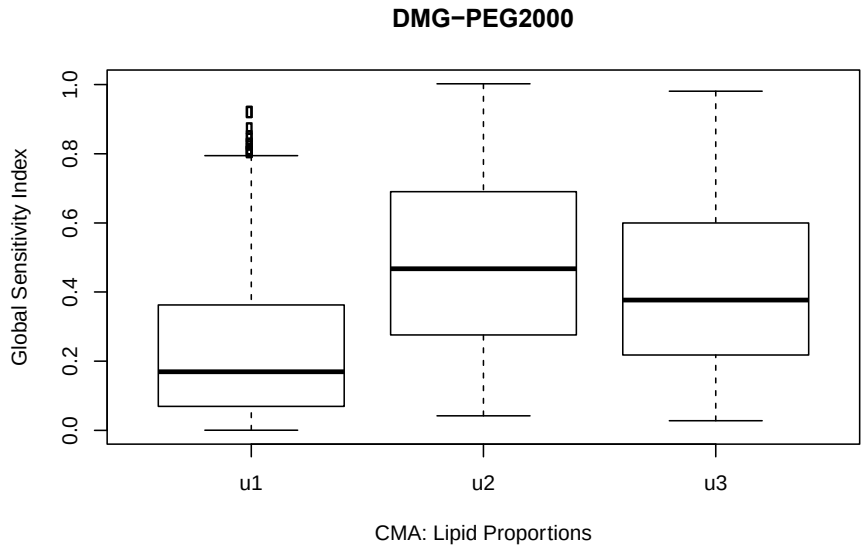

B

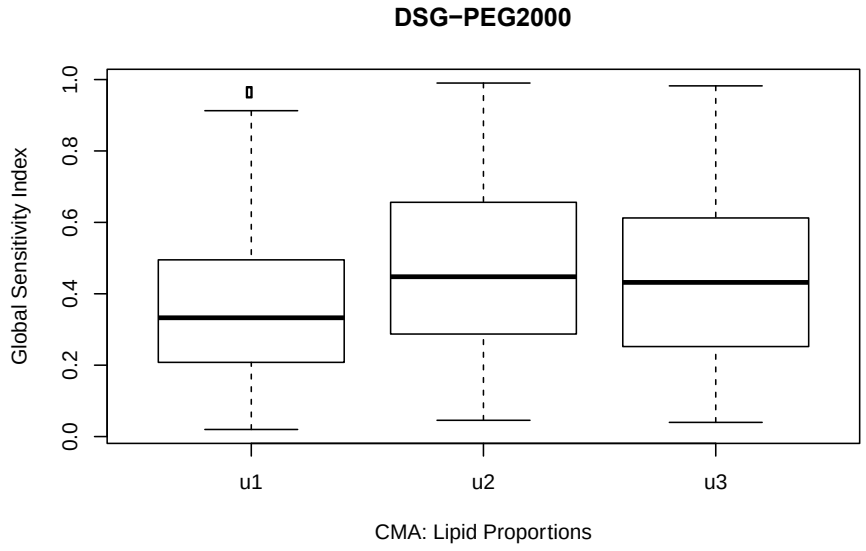

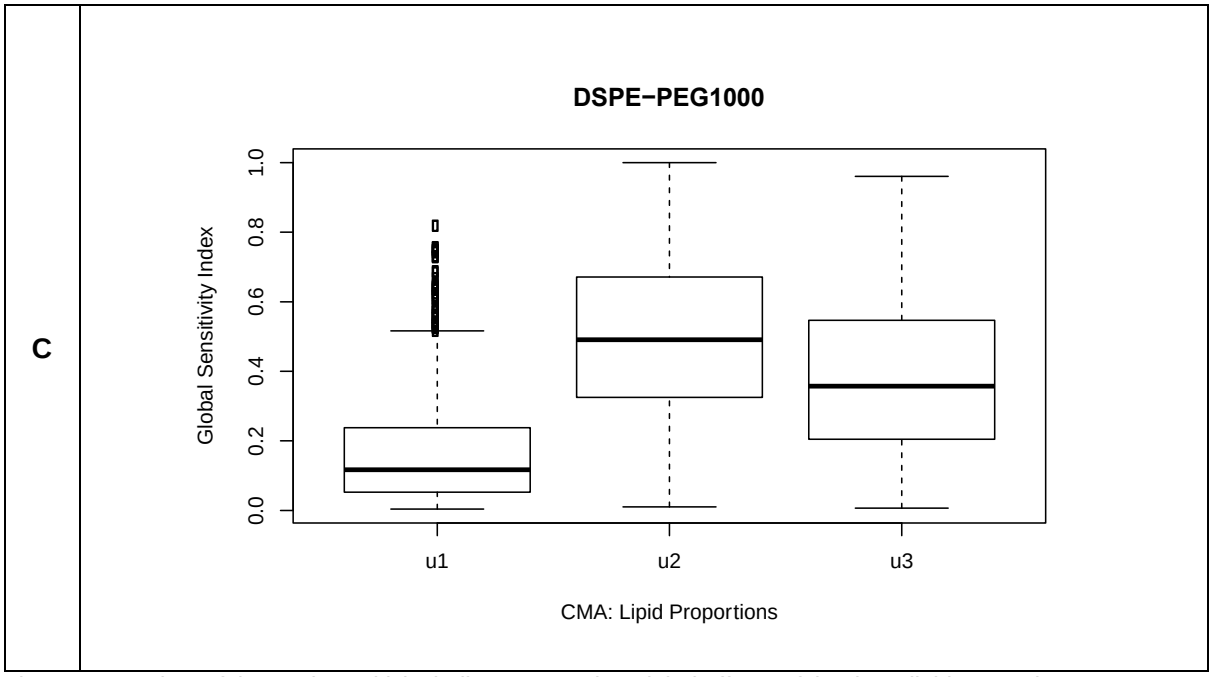

Figure 8: Boxplots of the total sensitivity indices comparing global effects of the three lipid proportions: %ionizable lipid (u_1), %PEG-lipid (u_2) and DOPE (u_3) on the %E7-specific T cell response. A: DMG-PEG2000, B: DSG-PEG2000 and C: DSPE-PEG1000. A boxplot is a standardized way of displaying the dataset based on a five-number summary: the minimum, the maximum (two whiskers), the sample median (horizontal bold black bar), and the first and third quartiles (box). Dots correspond to values estimated as outliers.

For DMG-PEG2000 based LNPs (Fig. 8A), estimated values of mean global sensitivity indices are: S1≈21% for u1, S2≈42% for u2 and S3≈ 37% for u3. For DSG-PEG2000 based LNPs (Fig. 8B), estimated values of mean global sensitivity indices are: S1≈27% for u1, S2≈37% for u2 and S3≈ 36% for u3. For DSPE-PEG1000 based LNPs (Fig. 8C), estimated values of mean global sensitivity indices are: S1≈16% for u1, S2≈49% for u2 and S3≈ 35% for u3.

Regardless of what type of PEG lipid was incorporated in the LNPs, we systematically observed that the T cell response is most sensitive to changes in %PEG-lipid, followed by changes in %DOPE and %ionizable lipid respectively. Changes in %ionizable lipid have a bigger mean impact on T cell response for DSG-PEG2000 LNPs (S= 27%) than for DMG-PEG-2000 (S=21) and DSPE-PEG1000 LNPs (S=16). The ratio of T cell response sensitivity to changes in %PEG-lipid over changes in %ionizable lipid is highest for DSPE-PEG1000LNPs (49/16 = 3), followed by DMG-PEG2000 (42/21 =2) and DSG-PEG2000 (37/27=1.4). We observe a quasi-constant sensitivity of the immune response with respect to %DOPE (around 36%), only the ratio %PEG-lipid/%ionizable lipid depends on the PEG-lipid type.

Response Prediction

After the qualification of the models for all three PEG-lipid types, we used the models to predict mean responses (%) for all combinations of the three factors (%ionizable lipid, %PEG-lipid, %DOPE). All predictions are gathered in Figure 9. The green region corresponds to the set of lipid proportions predicted to lead to the highest %E7-specfic T cell repsonse.

A	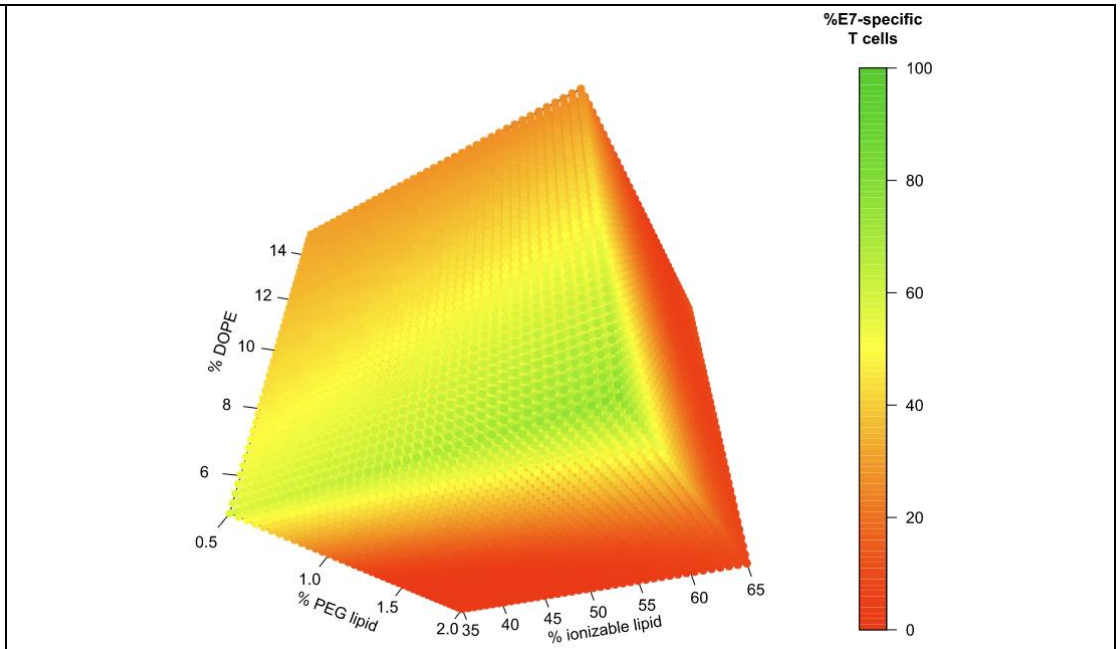
B	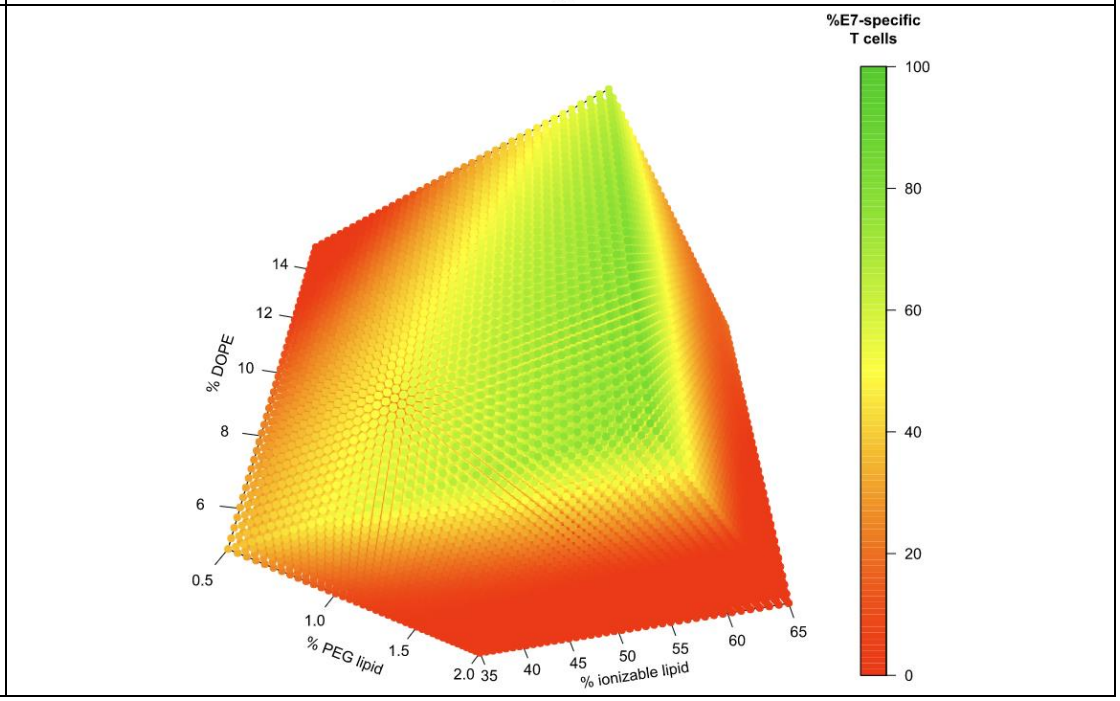

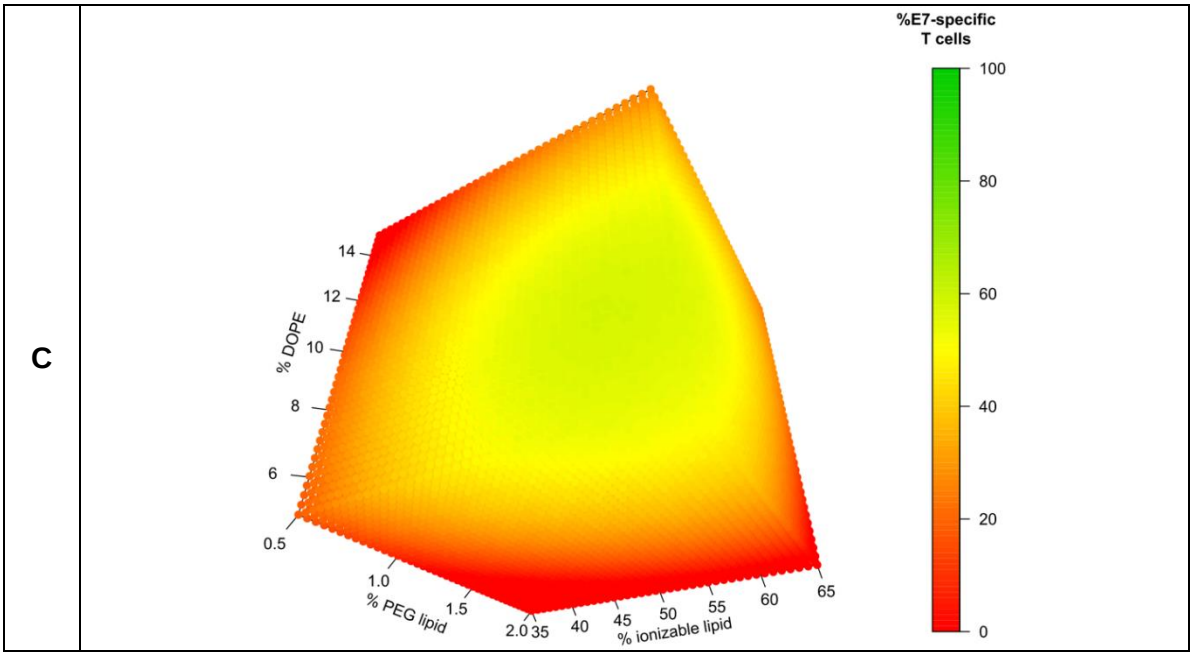

Figure 9: 3D model of mean predictions of the %E7-specific T cells in respect to %ionizable lipid, %PEG-lipid and DOPE. A: DMG-PEG2000, B: DSG-PEG2000 and C: DSPE-PEG1000.

For all PEG-lipid types, the optimal response region corresponds to high percentage of ionizable lipid and small percentages of PEG-lipid and DOPE.

Design Space (Risk mapping)

A Design Space is a multidimensional risk mapping in which probabilities to fulfill CQA specifications are split up into three regions: NOR (Normal Operating Region), PAR (Proven Acceptance Region) and OOS (Out Of Specification) denoting respectively: the desired region of interest, the domain where the product is still acceptable but corrections should be made and the area where the level of risk is not acceptable. In this study, region NOR has a probability to respect the specification of at least 50% E7-specific T cells greater than 90%. Region PAR has a probability between 70% and 90% while the last region, OOS has a probability lower than 70% to respect the specification. In practice, design spaces were determined from simulations carried out from posterior predictive distributions of the CD8 T cell response. Those response distributions were themselves obtained using Hamiltonian Monte Carlo, a family of Markov chain Monte Carlo (MCMC) algorithms.[10] Design spaces for each PEG-lipid type are given in Figure 10.

A	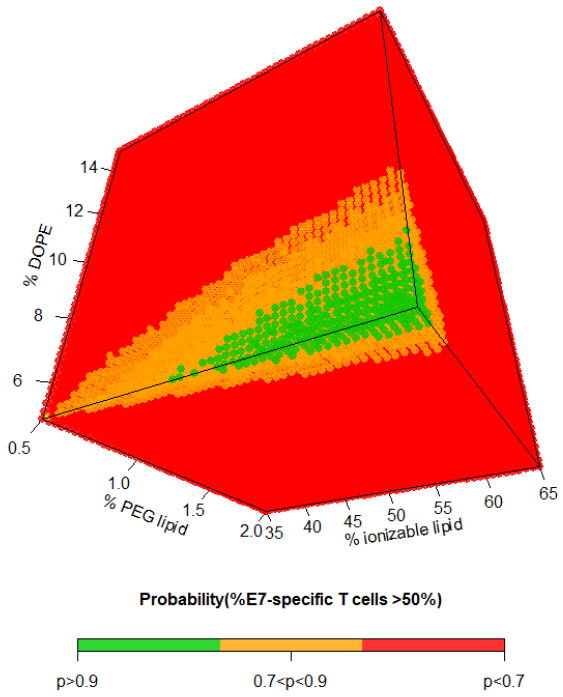 % DOPE 14 12 10 8 6 0.5 1.0 1.5 2.0 % PEG lipid 35 40 45 50 55 60 65 % ionizable lipid Probability(%E7-specific T cells >50%) p>0.9 0.7<p<0.9 p<0.7
B	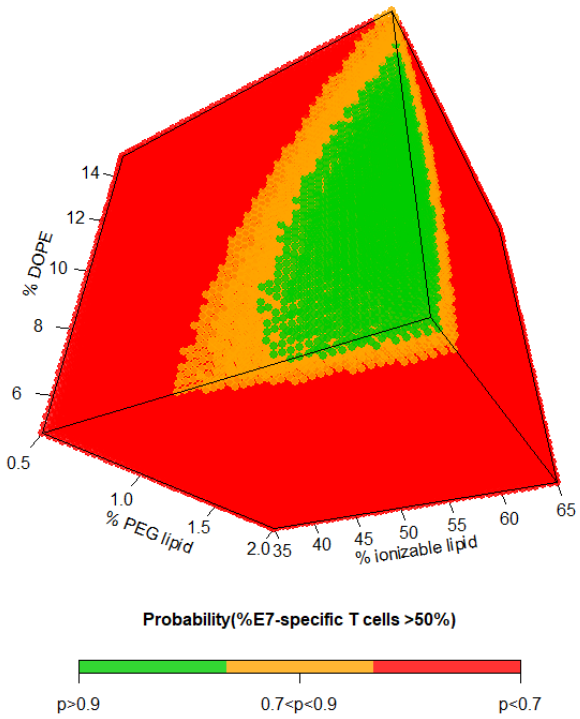 % DOPE 14 12 10 8 6 0.5 1.0 1.5 2.0 % PEG lipid 35 40 45 50 55 60 65 % ionizable lipid Probability(%E7-specific T cells >50%) p>0.9 0.7<p<0.9 p<0.7

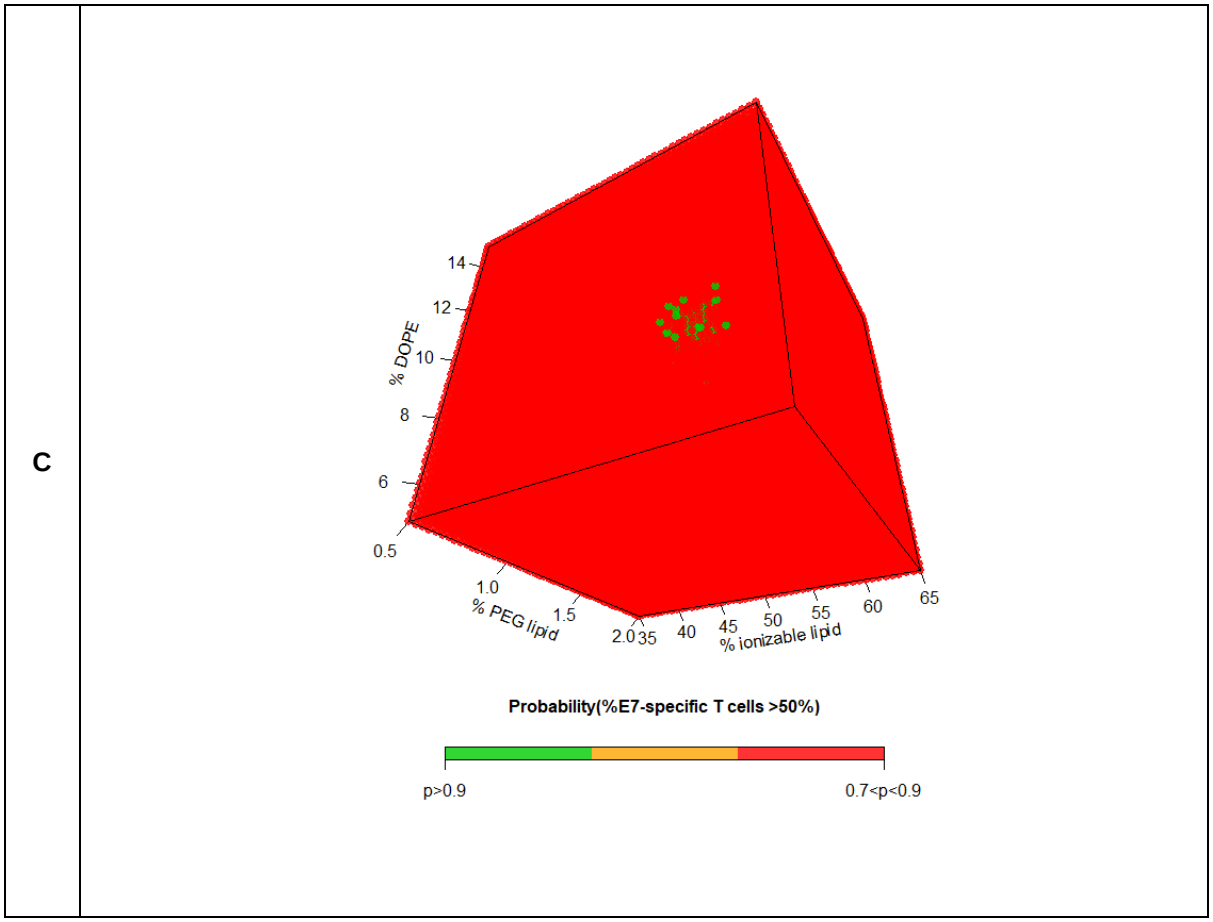

Figure 10: Design Spaces for DMG PEG2000 (A), DSG PEG2000 (B) and DSPE PEG-1000 (C). Green: NOR (Normal Operating Region), Orange: PAR (Proven Acceptance Region) and Red: OOS (Out Of Specification)

Risk assessment of the optimal LNP compositions

Based on the models described above, for each PEG-lipid a predicted optimal and predicted suboptimal LNP composition was chosen (LNPs 34-39), different from the compositions in the initial LNP library, and tested in 4-5 mice each. Table 4 presents the results of this cross-validation test. Four measured T cell responses out of 26 were out of the 95% confidence interval, which is acceptable in this *in vivo* context despite some gaps between predicted and observed mean values of the E7-specific T cells response.

		Lipid proportion (%)				Predicted E7-specific T cells (%)		Observed E7-specific T cells (%)	
PEG-lipid type	**LNP number**	**Ionizable lipid**	**DOPE**	**Cholesterol**	**PEG-lipid**	**Mean**	**95% confidence interval**		**Mean**
DMG-PEG2000	34	56.5	5.25	37.75	0.5	70	[43;95]	40, 67, 62, 57	59
	35	42	12	44.5	1.5	3	[0;21]	8, 4, 8, 10	8
DSG-PEG2000	36	64.4	8	27.1	0.5	82	[51;100]	65, 41, 53, 52	53
	37	42	12	44.5	1.5	6	[0 ;28]	7, 16, 1, 9, 3	8
DSPE-PEG1000	38	64.6	6.6	28.3	0.52	56	[15 ;95]	84, 36, 48, 49, 50	54
	39	42	12	44.5	1.5	26	[0 ;54]	61, 44, 38, 59, 54	51

Table 4: LNP compositions selected for the three types of PEG-lipid with their predicted responses (mean values and 95% confidence interval).

References

(1) *Committee for Human Medicinal Products, "ICH Guideline Q8 (R2) on Pharmaceutical Development," Tech. Rep. Step 5, European Medicine Agency, June 22 2017*.

(2) Hornik, K. The Comprehensive R Archive Network. *Wiley Interdisciplinary Reviews: Computational Statistics*. **2012**. https://doi.org/10.1002/wics.1212.

(3) Gelman, A.; Carlin, J. B.; Stern, H. S.; Dunson, D. B.; Vehtari, A.; Rubin, D. B. *Bayesian Data Analysis*; **2013**. https://doi.org/10.1201/b16018.

(4) Gabry, J.; Simpson, D.; Vehtari, A.; Betancourt, M.; Gelman, A. Visualization in Bayesian Workflow. *J. R. Stat. Soc. Ser. A Stat. Soc.* **2019**. https://doi.org/10.1111/rssa.12378.

(5) Gelman, A.; Goodrich, B.; Gabry, J.; Vethari, A. R-Squared for Bayesian Regression Models - The Problem Defining R 2 Based on the Variance of Estimated Prediction Errors. *Am. Stat.* **2018**.

(6) Wellek, S. A Critical Evaluation of the Current "p-Value Controversy." *Biometrical Journal*. **2017**. https://doi.org/10.1002/bimj.201700001.

(7) Wasserstein, R. L.; Lazar, N. A. The ASA's Statement on p-Values: Context, Process, and Purpose. *American Statistician*. **2016**. https://doi.org/10.1080/00031305.2016.1154108.

(8) Kuffner, T. A.; Walker, S. G. Why Are P-Values Controversial? *Am. Stat.* **2019**. https://doi.org/10.1080/00031305.2016.1277161.

(9) Salteli, A.; Ratto, M.; Andres, T.; Campolongo, F.; Cariboni, J.; Gatelli, D.; Saisana, M.; Tarantola, S. Global Sensitivity Analysis. *Biometrics* **2009**, *65* (4), 1311–1312. https://doi.org/10.1111/j.1541-0420.2009.01343_7.x.

(10) Gelman, A.; Carlin, J. B.; Stern, H. S.; Dunson, D. B.; Vehtari, A.; Rubin, D. B. *Bayesian Data Analysis, Third Edition*; 2013.

Supplementary Method: Adsorption of plasma proteins on LNPs

Incubation of LNPs with plasma

10 µl of LNPs (conc.=100 µg mRNA/ml) were mixed with 90 µl of 10% plasma in PBS adjusted to 10 mM sodium citrate to prevent coagulation. The mixure was incubated for 1 h at 37 ℃. The LNP-corona complexes were spun at 20,000 × g at 4 °C for 1h, supernatant discarded, and the pellet resuspended in 100 µl PBS. The LNP-corona pellet was washed twice with PBS using the same procedure then resuspended in 20 µl PBS and protein content was measured using Micro BCA™ protein assay kit (ThermoFisher, USA).

Sample preparation for proteomics

Proteins (3 µg) were precipitated with the trichloroacetic acid deoxycholate (TCA/DOC) method, as described elsewhere [1]. Protein pellets were suspended in 7 M urea / 2 M thiourea, 100 mM ABC, 20 mM methylamine solution, followed by disulfide reduction and cysteine alkylation with 5 mM DTT and 10 mM chloroacetamide for 60 min each at room temperature. Proteins were predigested with 1:50 (enzyme to protein) Lys-C (Wako Chemicals) for 4 h, diluted 5 times with 100 mM ABC and further digested with trypsin (Sigma Aldrich) overnight at room temperature. Peptides were desalted with in-house made C18 StageTips.

Nano-LC/MS/MS measurement

Samples were injected to an Ultimate 3000 RSLCnano system (Dionex) using a C18 trap-column (Dionex) and an in-house packed (3 µm C18 particles, Dr Maisch) analytical 50 cm x 75 µm ID emitter-column (New Objective). Peptides were eluted at 200 nl/min with a 8-40% B 120 min gradient (buffer B: 80% acetonitrile + 0.1% formic acid, buffer A: 0.1% formic acid) to a Q Exactive Plus (Thermo Fisher Scientific) mass spectrometer (MS) using a nano-electrospray source (spray voltage of 2.5 kV). The MS was operated with a top-10 data-dependent acquisition strategy. Briefly, one 350-1400 m/z MS scan at a resolution setting of R=70 000 at 200 m/z was followed by higher-energy collisional dissociation fragmentation (normalized collision energy of 26) of 10 most intense ions (z: +2 to +6) at R=17 500. MS and MS/MS ion target values were 3e6 and 5e4 with 50 ms injection times. Dynamic exclusion was limited to 40 s.

Raw Data Processing

Mass spectrometric raw files were analyzed the with the MaxQuant software (version 1.6.15.0) [2]. Methionine oxidation and protein N-terminal acetylation were set as variable modifications, while cysteine carbamidomethylation was defined as a fixed modification. Search was performed against UniProt (www.uniprot.org) *Mus musculus* reference proteome database (downloaded on 04.01.2021) using the tryptic digestion rule (including cleavages after proline). Only identifications with minimally 1 peptide 7 amino acids long were accepted and transfer of identifications between runs was enabled. Label-free normalization with MaxQuant LFQ algorithm was also applied. Protein and LFQ ratio count (i.e. number of quantified peptides for

reporting a protein intensity) was set to 1. Peptide-spectrum match and protein false discovery rate (FDR) was kept below 1% using a target-decoy approach. All other parameters were default.

Proteomics data analysis

Differential enrichment analysis was performed on the LFQ Intensity values by using Differential Enrichment analysis of Proteomics data (DEP) Version 1.10.0 [3], R Version 4.0.2 and RStudio version 1.3.1073. The figures were modified with GraphPad Prism Version 9 (GraphPad Software, Inc., La Jolla, CA, USA), if applicable.

References

(1) Using Deoxycholate and Trichloroacetic Acid to Concentrate Proteins and Remove Interfering Substances. *Cold Spring Harb. Protoc.* **2006**. https://doi.org/10.1101/pdb.prot4258.

(2) Cox, J.; Mann, M. MaxQuant Enables High Peptide Identification Rates, Individualized p.p.b.-Range Mass Accuracies and Proteome-Wide Protein Quantification. *Nat. Biotechnol.* **2008**, *26* (12), 1367–1372. https://doi.org/10.1038/nbt.1511.

(3) Zhang, X.; Smits, A. H.; Van Tilburg, G. B. A.; Ovaa, H.; Huber, W.; Vermeulen, M. Proteome-Wide Identification of Ubiquitin Interactions Using UbIA-MS. *Nat. Protoc.* **2018**, *13* (3), 530–550. https://doi.org/10.1038/nprot.2017.147.

Supplementary Method: TC-1 tumor experiment (Figure S2)

TC-1 cells were obtained from Leiden University Medical Center. 0.5 million TC-1 cells in 50 µl PBS were injected subcutaneously in the right flank of the mice. Tumor measurements were performed using a caliper. Tumor volume was calculated as (smallest diameter^2 x largest diameter)/2. At a mean tumor volume of 55mm^3, mice were injected i.v. via the tail vein with TBS or 5 µg of either E7-TriMix mRNA, Fluc-TriMix mRNA or Fluc mRNA in LNP36. Immunizations were performed weekly for a total of 3 times. At day 15 (n=4/group) and day 35 (n=6), tumors were isolated and placed in a 24-well plate filled with MACS tissue storage buffer (Miltenyi Biotec) for flow cytometry analysis.

Flow cytometry

Tumors were cut into 3mm^3 pieces and transferred to MACS C tubes containing digestion buffer prepared according to protocol of Tumor Dissociation Kit, mouse (Miltenyi Biotec). The content of enzyme R was reduced to 20% in the enzyme mix to help preserve cell surface epitopes. Single-cell suspensions were generated by use of a gentleMACS Octo dissociater (program 37C_m_TDK_2). Samples were immediately filtered through a 70 µm cell strainer, followed by lysis of red blood cells. Next, samples were split over two 96-well plates to stain with 2 different antibody cocktails. For both plates the cells were first incubated with FcR block and viability dye. After 20' incubation at 4°C both plates were washed. Next, an antibody mixture for surface molecules CD45, Thy1.2, CD19, MHCII, CD11c, CD11b, Ly6G, F4/80 and CD206 (Table S3) was added to the cells of plate 1 and incubated for 30 minutes at 4 °C. To plate 2, APC labelled E7 (RAHYNIVTF)-tetramer was added and incubated at RT for 30 minutes. Hereafter, excess tetramer was washed away and an antibody mixture for surface molecules CD45, CD4, CD8 and PD-1 (Table S3) was added and incubated for 30 minutes at 4 °C. Excess antibodies were washed off. Before proceeding with intracellular staining, cells were fixated and permeabilized with FoxP3 Fixation/Permeabilization solution (eBioscience) according to manufacturer protocol. Cells were kept in Fixation/Permeabilization solution overnight at 4 °C. The next morning, cells were washed with permeabilization buffer followed by addition of an antibody mixture of FoxP3, granzyme B and Ki67 antibodies (in permeabilization buffer) (Table S3). Samples were acquired on a 3-laser AttuneNxt flow cytometer. Analysis was done using FlowJo software. Gating strategies are provided in the next section of Supplementary information.

RT-qPCR

Tumors of mice that had reached a volume of 1000 mm^3 (for TBS, Fluc-TriMix and Fluc groups, n=11-12) or tumors that had relapsed at day 35 (for the E7-TriMix group, n=3) were washed in MACS tissue storage buffer, blotted dry, snap-frozen in liquid nitrogen and stored at -80˚C. Pieces of approximately 100mg were cut off, weighed and mixed with 1 mL TRIzol Reagent per 100 mg tissue (Thermo Fisher Scientific) in tubes containing 1.4 mm ceramic beads (Qiagen). Tissues were homogenized for 60 seconds at 4°C in a a Mini-BeadBeater-8 (BioSpec) at full speed for 60s at 4˚C. Homogenates were stored at -20˚C, thawed, centrifuged at 10.000 x g for 10 min at 4˚C to remove beads and debris, and 500 µL of supernatants were transferred to clean tubes. Phase-separation and RNA isolation was carried out according to manufacturer's instructions. RNA was dissolved in 150 µL nuclease-free water (Ambion) and stored at -80°C. Reverse transcription was performed using an iScript cDNA Synthesis Kit (Bio-Rad) in 10 µL reactions containing 375ng of RNA according to manufacturer's instructions. Resulting cDNA was diluted with 90 µL of nuclease-free water. Three microliters of each sample were used as input for 10 µL reactions containing 1X iQ™ SYBR® Green Supermix (Bio-Rad) and 250 nM of forward and reverse primers. Reactions were run on a CFX96 Touch Real-Time thermocycler (Bio-Rad) using the following cycling parameters: 3 min 95°C, 45 cycles of 40s 60°C and 15s 95°C, followed by melting curve analysis. Ct values of E7 and housekeeping gene beta-2-microglobulin (B2m)

were converted to fold changes compared to TBS-treated mouse values using the ΔΔCt method. Primer sequences were

E7_Fw: 5’- TCAGAGGAGGAGGATGAAATAGATGGTC-3',
E7_Rv: 5’- GCACAACCGAAGCGTAGAGTCAC-3',

Supplementary Method: Ex vivo LNP opsonization experiment

LNP34 and LNP36 were formulated with Fluc mRNA and Cy5-Fluc mRNA in a 1:9 ratio and diluted to an mRNA concentration of 0.1 mg/mL. Twenty-five microliters of each LNP were mixed with 1µg of rabbit anti-PEG IgG (Abcam, clone RM105) and incubated for 30 min at room temperature. LNPs were then mixed with 100 µL of pooled mouse serum obtained from wild-type C57Bl/6 mice and incubated for 30 or 120 min at 37°C. Mixtures were loaded onto a XK16/20 column (Cytiva) packed with Sepharose CL-4B resin equilibrated with PBS. Size exclusion chromatography (SEC) was performed using a refrigerated ÄKTA Start chromatography system (Cytiva) at a flow rate of 1 mL/min, while 1mL fractions were collected. LNP-containing fractions were pooled and aliquots were analysed by Dynamic Light Scattering as described in the main text. As controls for proper separation of LNPs and unbound anti-PEG, anti-PEG was incubated with serum in the absence of LNPs, subjected to SEC and typical LNP-containing fractions were collected. All samples were concentrated on Amicon Ultra-4 Centrifugal Filter Units with 100 kD molecular weight cut-off to volumes of approximately 50µL. LNP concentrations were normalized based on Cy5 fluorescence, which was measured using a SpectraMax iD3 platereader (Molecular Devices). Equal quantities of LNP-derived fluorescence were mixed with sample buffer containing dithiothreitol (DTT), heated to 95°C for 10 min, and subjected to SDS-PAGE using 4-12% Bis-Tris polyacrylamide gels (Thermo Fisher Scientific). Proteins were electrotransferred to Immobilon-FL polyvinylidene difluoride (PVDF) membranes (Merck Millipore). Membranes were blocked, probed with IRDye® 800CW Goat anti-Rabbit IgG secondary antibodies (LI-COR) and imaged using an Odyssey M Imaging System (LI-COR). Band intensities were quantified using Emperia Studio 2.1 (LI-COR).

Supplementary Method: Flow cytometry gating strategies

Flow cytometry gating strategies of all stainings performed in this work. Clone and catalog numbers of the used antibodies are summarized in Supplementary table 3.

Gating strategy of spleens (wild-type mice) to determine cellular Cy5-mRNA association

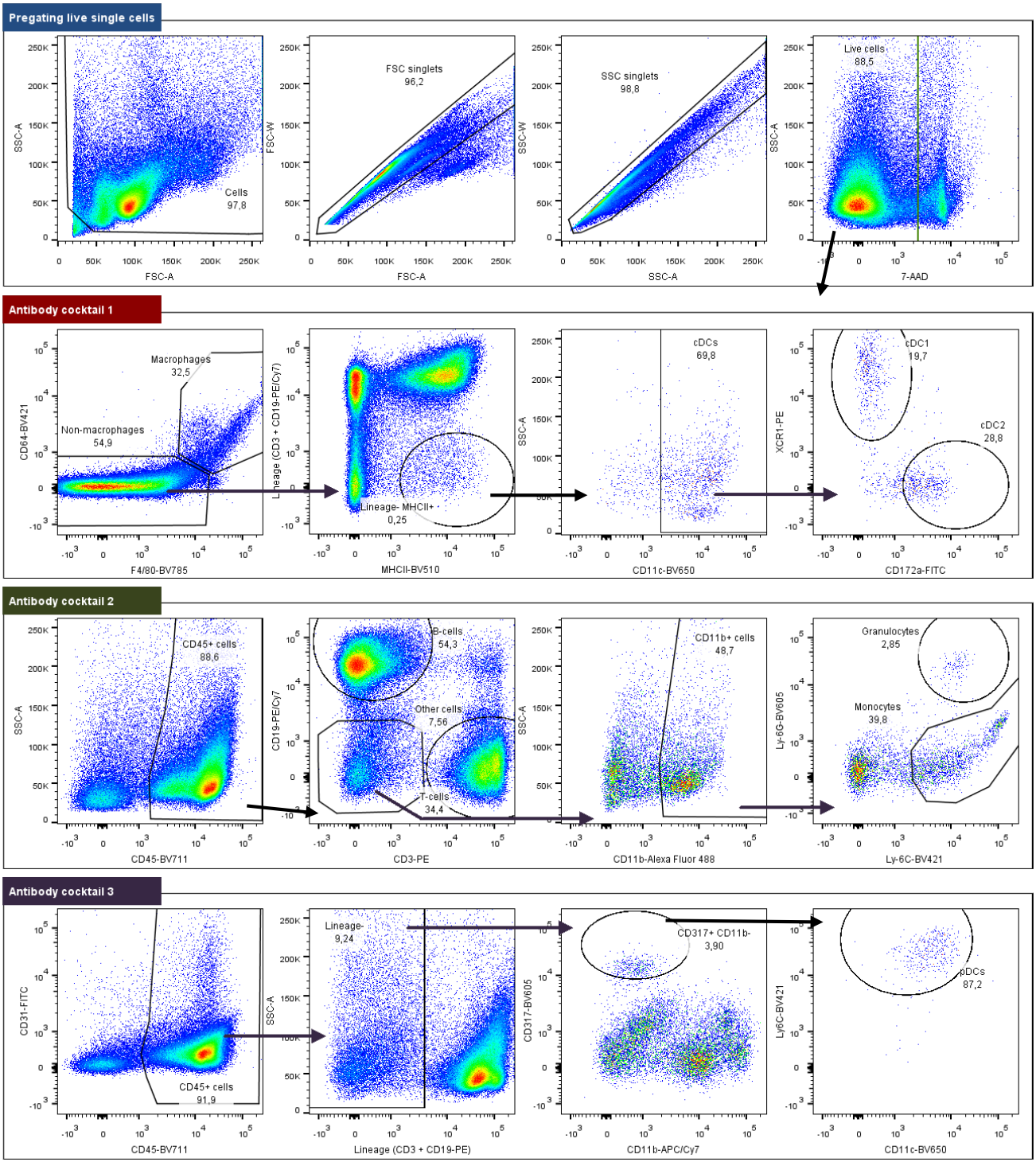

Gating strategy of livers (wild-type mice) to determine cellular Cy5-mRNA association

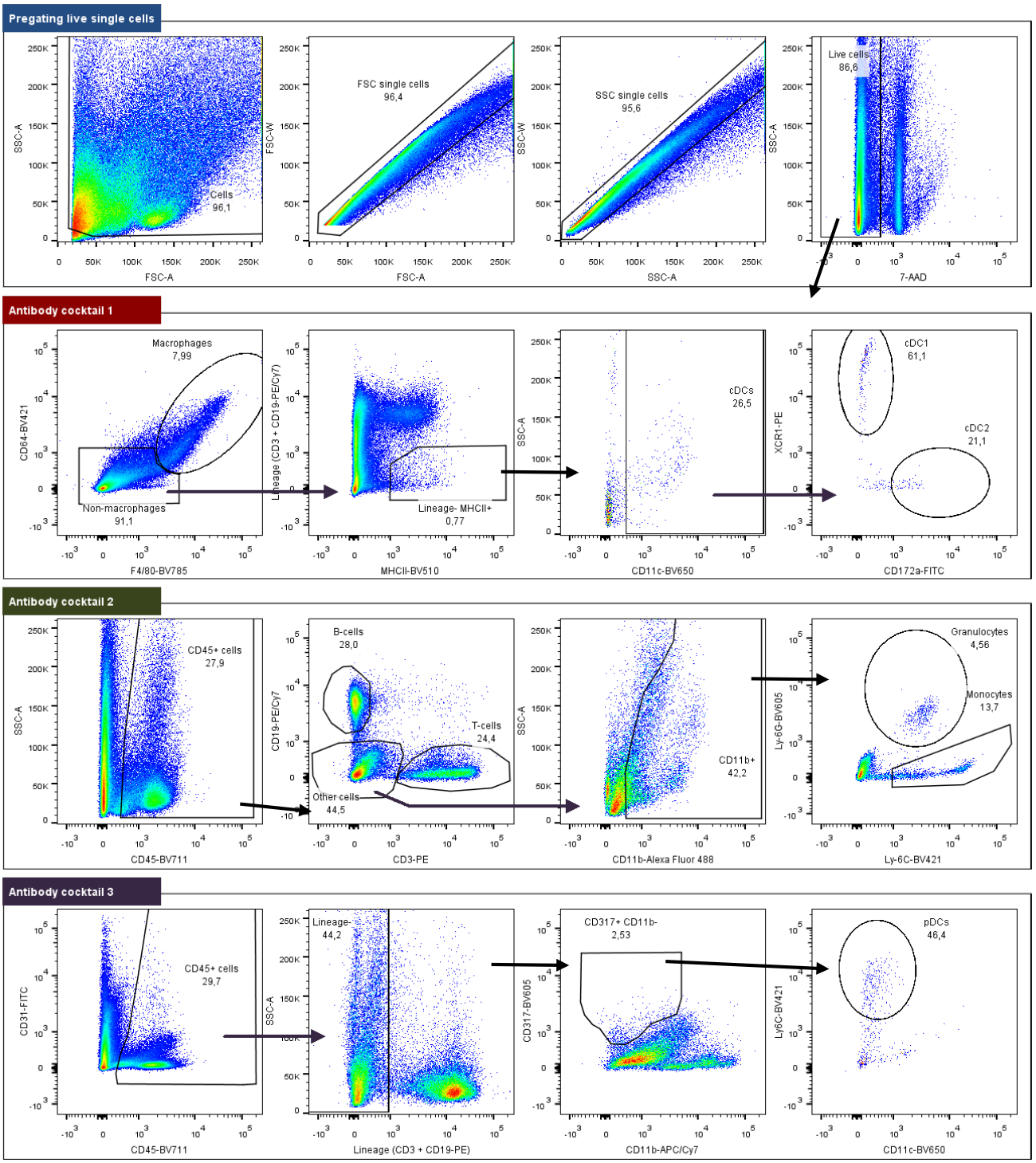

Gating strategy of spleens (Ai9; Cre reporter mice) to determine cellular tdTomato expression

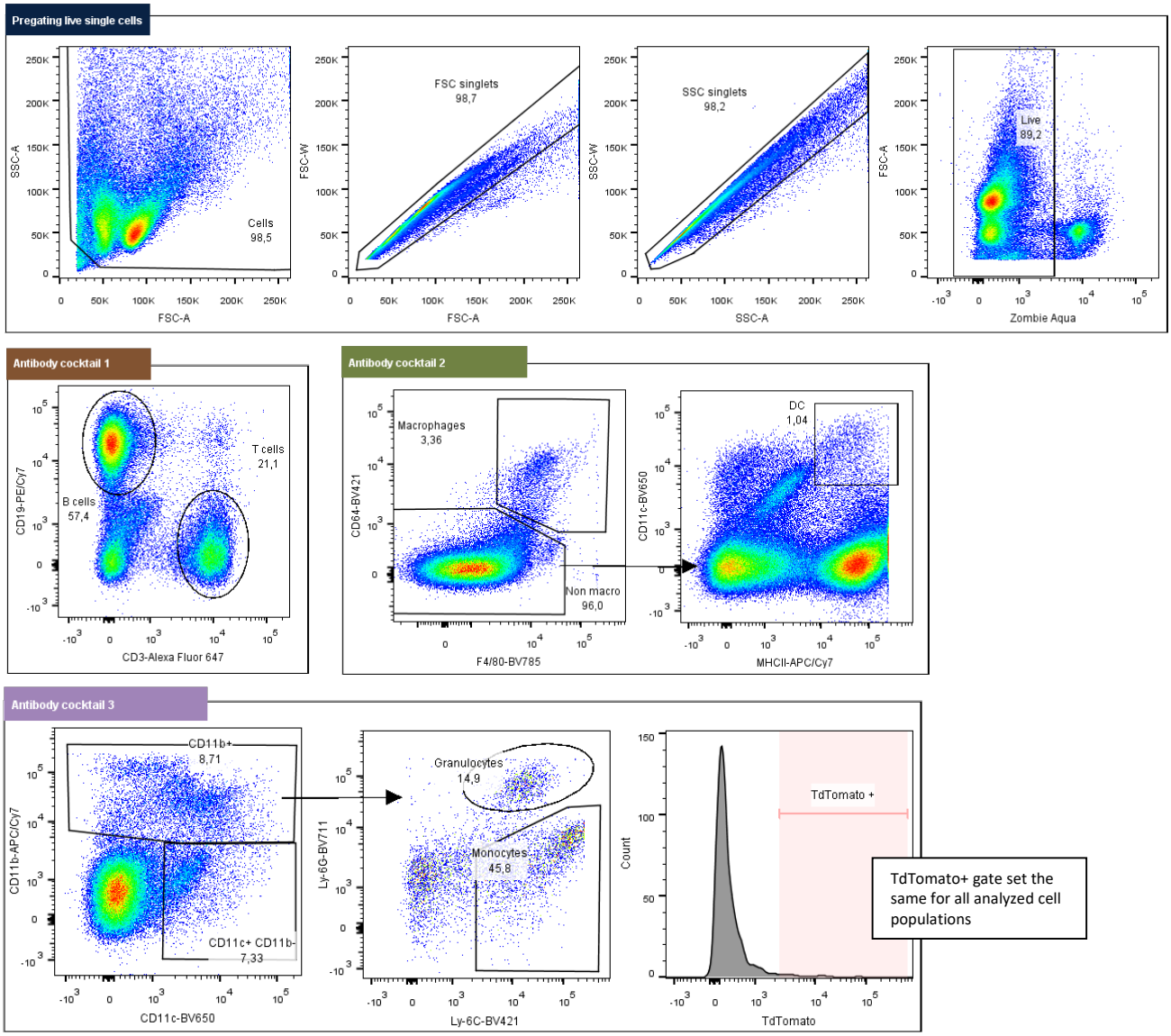

Gating strategy of CD8 T cells in mouse blood to determine E7-specificity and phenotype

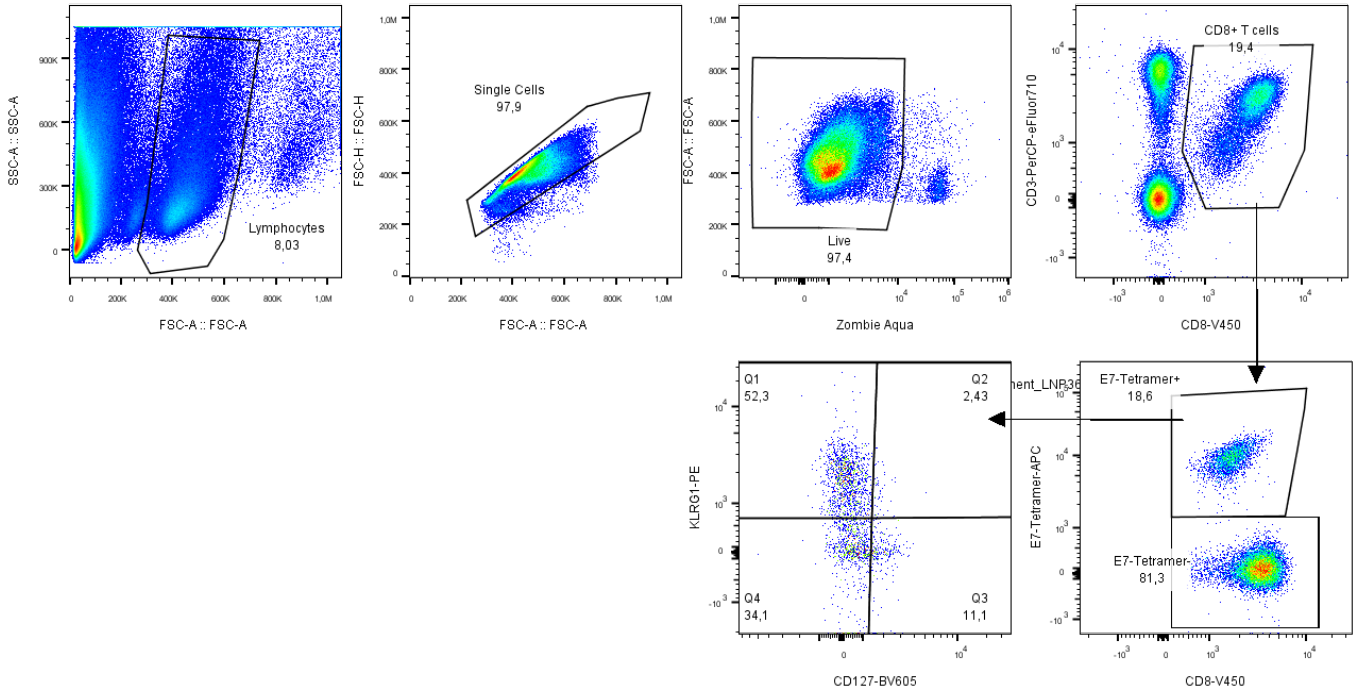

Gating strategy of spleens (wild-type mice) to determine activation status of B cells

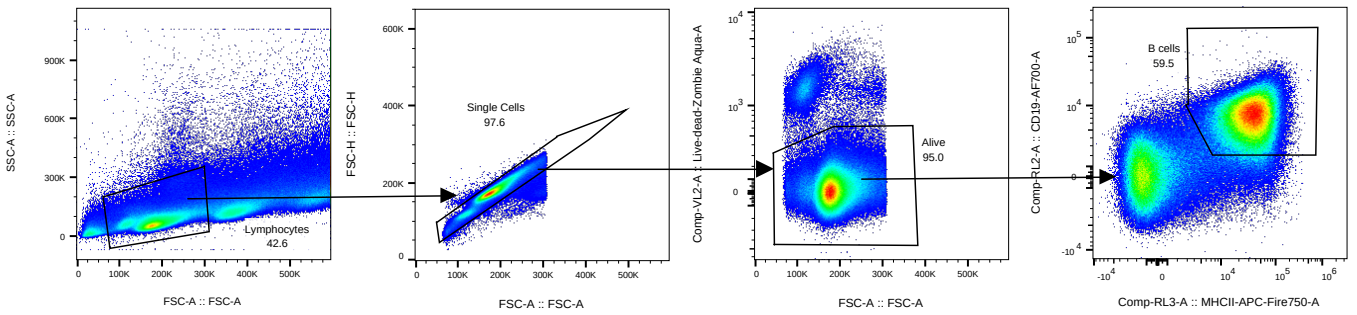

Gating strategy of spleens (wild-type mice) to determine activation status of cDC1 and cDC2

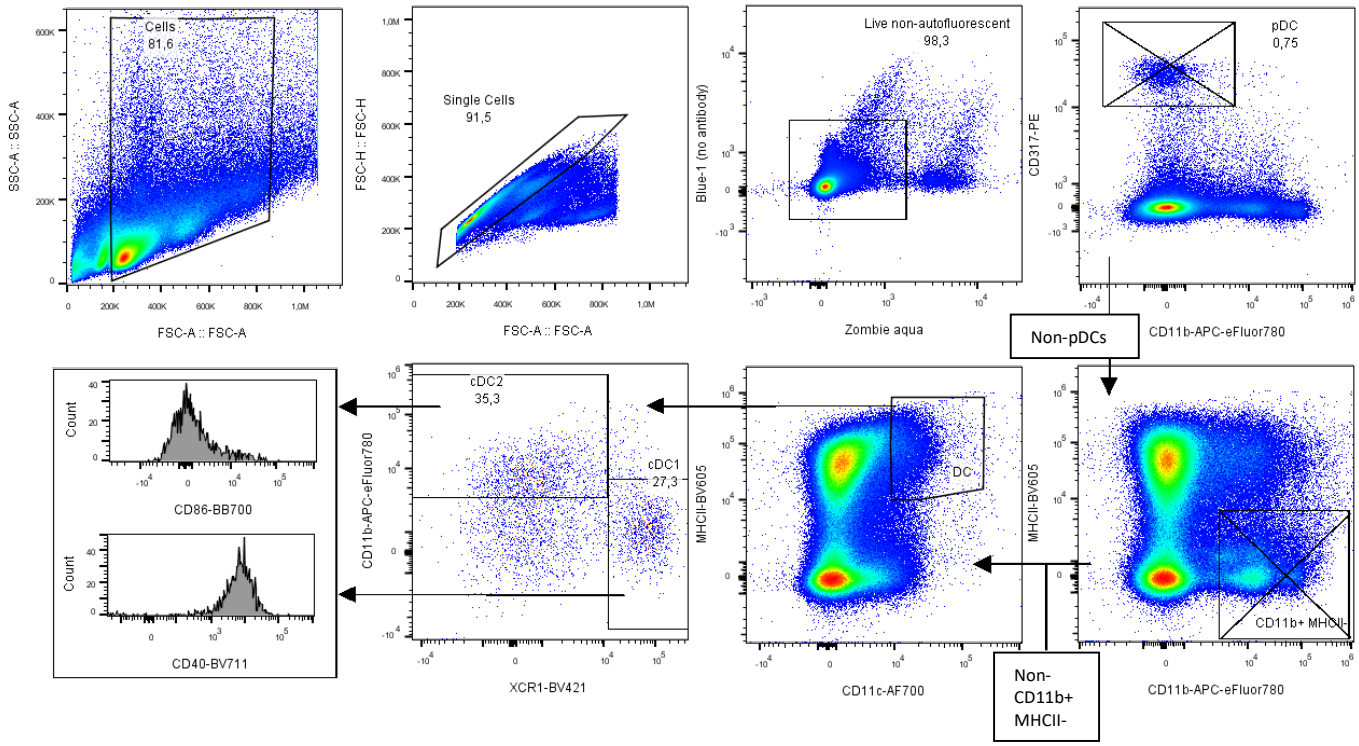

Gating strategy of spleens (wild-type mice) to determine CD8 T cell cytokine secretion

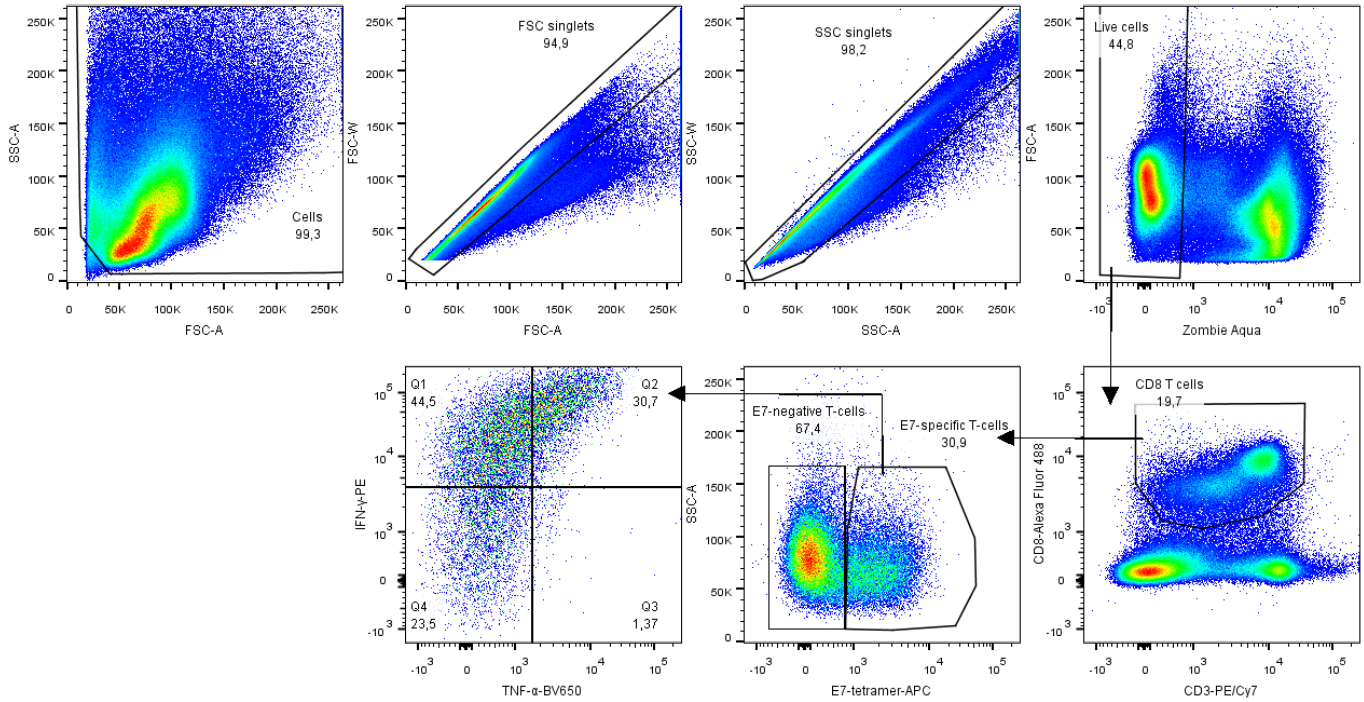

Gating strategy of TC-1 tumors to quantify infiltrating CD8 T cells (for figure 2)

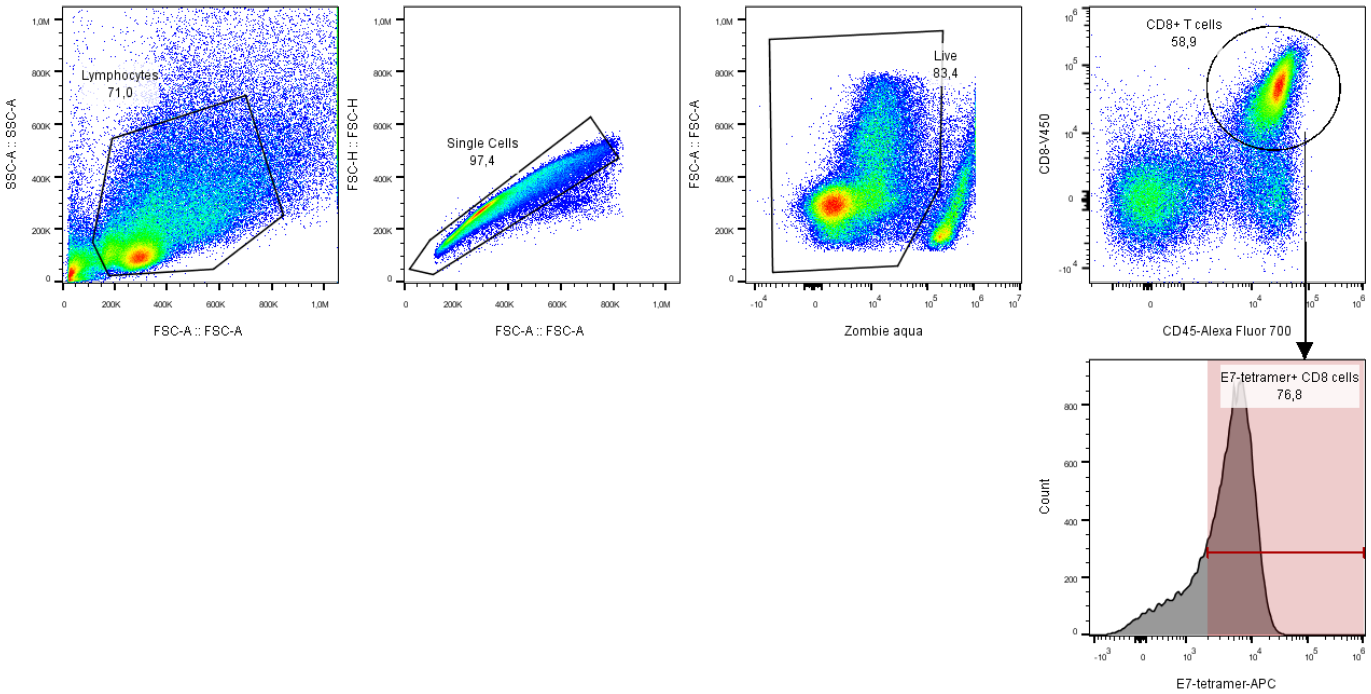

Gating strategy of TC-1 tumors to quantify and characterize infiltrating CD8 T cells (for figure S2)

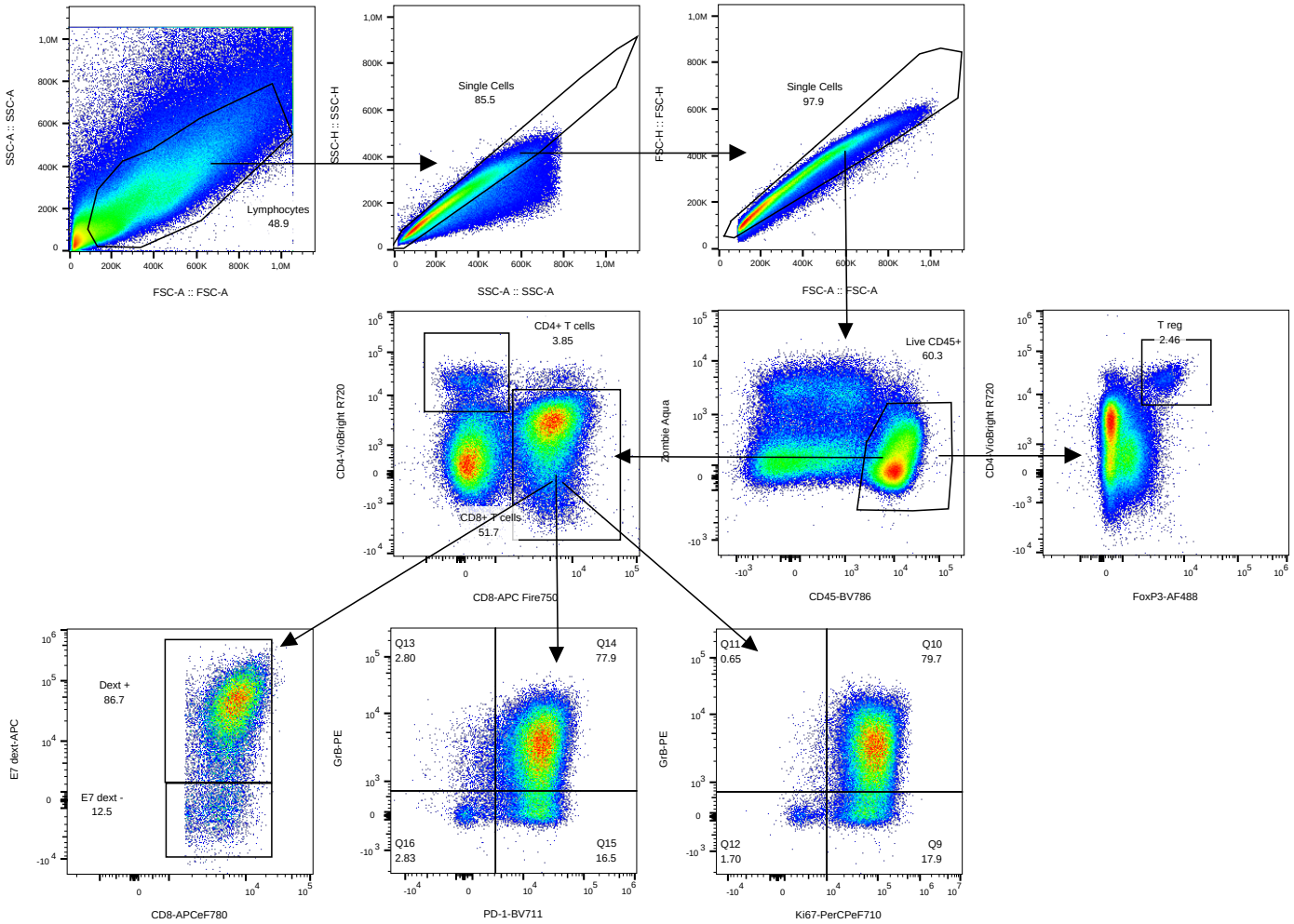

Gating strategy of TC-1 tumors to quantify infiltrating immune cells (for figure S2)

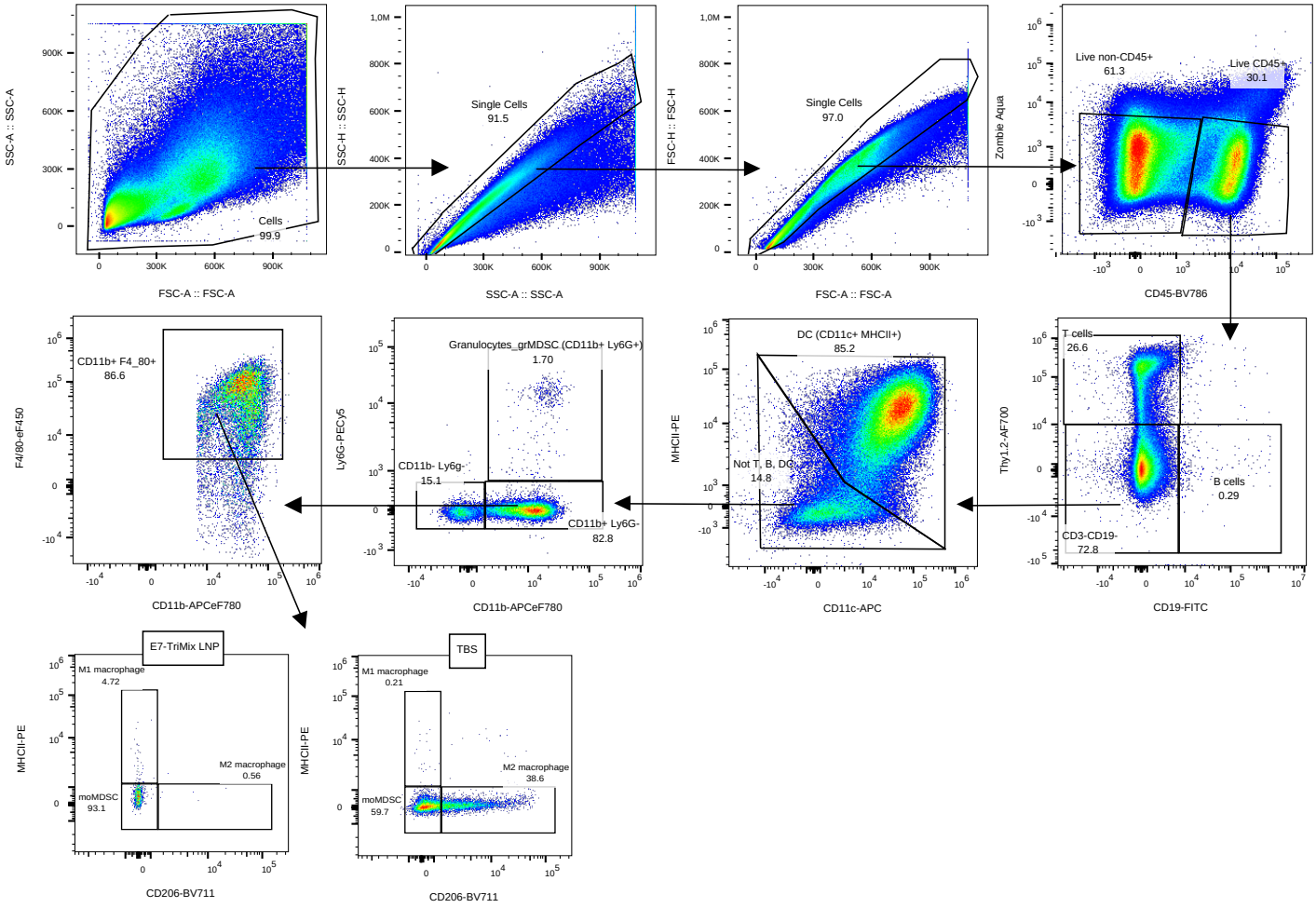

Supplementary Tables

Table S1. LNP properties

Lipid composition (molar percentages), size, polydispersity index (PDI), %mRNA encapsulation and zeta potential of all LNPs used in this work.

		Composition (molar %)						Size (nm)	PDI	%mRNA encapsulation	Zeta potential (mV)
Library	LNP number	SS-EC	DOPE	Cholesterol	DMG-PEG2000	DSG-PEG2000	DSPE-PEG1000				
DOE	1	50	15	33.75	1.25			73	0.12	97	4
	2	50	5	43.75	1.25			86	0.09	96	-2
	3	40.5	12.24	46.48	0.78			89	0.09	96	0
	4	59.5	12.24	27.48	0.78			107	0.07	94	5
	5	40.5	12.24	45.54	1.72			66	0.14	97	1
	6	59.5	12.24	26.54	1.72			83	0.12	97	3
	7	36.6	7.76	54.39	1.25			71	0.09	97	-1
	8	63.4	7.76	27.59	1.25			112	0.09	96	7
	9	50	7.76	41.66	0.58			111	0.09	95	-3
	10	50	7.76	40.32	1.92			76	0.15	96	0
	11	50	10	38.75	1.25			83	0.08	97	2
	12	50	15	33.75		1.25		80	0.13	97	4
	13	50	5	43.75		1.25		93	0.07	96	-1
	14	40.5	12.24	46.48		0.78		92	0.07	95	-1
	15	59.5	12.24	27.48		0.78		128	0.08	93	4
	16	40.5	12.24	45.54		1.72		66	0.09	97	0
	17	59.5	12.24	26.54		1.72		93	0.07	96	3
	18	36.6	7.76	54.39		1.25		78	0.10	97	-2
	19	63.4	7.76	27.59		1.25		123	0.05	76	-2
	20	50	7.76	41.66		0.58		116	0.07	94	-3
	21	50	7.76	40.32		1.92		82	0.11	96	1
	22	50	10	38.75		1.25		87	0.07	96	2
	23	50	15	33.75			1.25	95	0.08	93	0
	24	50	5	43.75			1.25	99	0.07	94	-4
	25	40.5	12.24	46.48			0.78	118	0.07	92	-8
	26	59.5	12.24	27.48			0.78	135	0.07	89	-1
	27	40.5	12.24	45.54			1.72	81	0.10	96	-7
	28	59.5	12.24	26.54			1.72	98	0.09	95	1
	29	36.6	7.76	54.39			1.25	100	0.05	91	-8
	30	63.4	7.76	27.59			1.25	133	0.02	94	-1
	31	50	7.76	41.66			0.58	163	0.06	89	-7
	32	50	7.76	40.32			1.92	88	0.13	93	-4
	33	50	10	38.75			1.25	100	0.07	94	-6
Validation	34	56.49	5.25	37.76	0.5			122	0.05	97	-8
	35	42	12	44.5	1.5			68	0.13	99	-3
	36	64.41	7.97	27.12		0.5		136	0.06	96	-4
	37	42	12	44.5		1.5		70	0.12	99	-4
	38	64.59	6.62	28.27			0.52	153	0.07	89	-7
	39	42	12	44.5			1.5	79	0.08	90	-15

Table S2. Correlations between LNP size, T cell response and splenic expression.

Significant positive or negative correlations as assesed by Pearson correlation test are marked in green or red respectively. Significant positive correlations were present between LNP size and %E7-specific T cells in blood after 3 weekly immunizations with E7 mRNA encapsulating DMG-PEG2000 or DSG-PEG2000 LNPs. In addition, LNP size significantly correlated with relative expression in the spleen (as % of total luciferase activity in all analyzed organs) 4h after single administration of Fluc mRNA LNPs. The %E7-specific T cell response (3 immunizations) moreover significantly correlated with relative (DMG-PEG2000) or absolute (DSG-PEG2000) fluc mRNA expression (1 administration) in spleen, whereas there is no correlation with total mRNA expression and a negative correlation with mRNA expression in liver.

DMG-PEG2000 LNPs

		%E7-specific T cells	Relative spleen luciferase activity
LNP size	Pearson r	0.910	0.944
	p value	1.03E-04	1.26E-05
Relative spleen luciferase activity	Pearson r	0.691	
	p value	0.019	
Absolute spleen luciferase activity	Pearson r	0.286	
	p value	0.394	
Relative liver luciferase activity	Pearson r	-0.685	
	p value	0.020	
Absolute liver luciferase activity	Pearson r	-0.520	
	p value	0.101	
Total luciferase activity	Pearson r	-0.457	
	p value	0.158	

DSG-PEG2000 LNPs

		%E7-specific T cells	Relative spleen luciferase activity
LNP size	Pearson r	0.805	0.667
	p value	0.003	0.025
Relative spleen luciferase activity	Pearson r	0.262	
	p value	0.436	
Absolute spleen luciferase activity	Pearson r	0.888	
	p value	3.00E-04	
Relative liver luciferase activity	Pearson r	-0.201	
	p value	0.553	
Absolute liver luciferase activity	Pearson r	0.166	
	p value	0.627	
Total luciferase activity	Pearson r	0.289	
	p value	0.389	

Table S3. Flow cytometry antibodies used in this work
List of all antibodies, including clone number, catalog number and manufacturer, used for flow cytometry analyses.

Name	Fluorophore	Manufacturer	Clone
Live/Dead	Zombie Aqua	BioLegend	-
Live/Dead	Zombie NIR	BioLegend	-
Live/Dead	7-AAD		-
CD16/32 (Fc block)	-	BD	2.4G2
CD16/32 (Fc block)	-	Biolegend	93
E7-Tetramer	APC	MBL International	-
CD11c	AF700	BD Biosciences	HL3
CD11c	BV650	BD Biosciences	HL3
CD11c	BV650	BioLegend	N418
CD11c	APC	BioLegend	N418
CD127	BV605	BioLegend	A7R34
CD11b	APC-eF780	Invitrogen	M1/70
CD11b	AF488	eBioscience	M1/70
CD11b	APC-Cy7	BioLegend	M1/70
CD172a	FITC	BioLegend	P84
CD19	FITC	BD Biosciences	1D3
CD19	AF700	BD Biosciences	1D3
CD19	FITC	BioLegend	6D5
CD19	PE-Cy7	BioLegend	6D5
CD19	PE	BioLegend	6D5
CD31	FITC	BD Pharmingen	MEC 13.3
CD317	PE	BioLegend	129C1
CD317	BV605	BioLegend	927
CD3	PerCPeF710	Invitrogen	17A2
CD3ε	FITC	BD Biosciences	145-2C11
CD3ε	PE-Cy7	BioLegend	145-2C11
CD3ε	PE	BioLegend	145-2C11
CD3ε	AF647	BioLegend	145-2C11
CD4	Viobright R720	Miltenyi Biotec	REA604
CD40	BV711	BD Biosciences	3/23
CD45	AF700	Invitrogen	30-F11
CD45	BV711	BioLegend	30-F11
CD45	BV786	BD Biosciences	30-F11
CD64	BV421	BioLegend	X54-5/7.1
CD69	BV650	BD Biosciences	H1.2F3
CD8	APC-Fire750	BioLegend	53-6.7
CD8	V450	BD Biosciences	53-6.7
CD86	BB700	BD Biosciences	GL1
CD206	BV711	BioLegend	C068C2
F4/80	eF450	Invitrogen	BM8
F4/80	BV785	BioLegend	BM8
FoxP3	AF488	Invitrogen	150D/E4
Granzyme B	PE	Invitrogen	GB12
IFN-γ	PE	BioLegend	4S.B3
Ki67	PerCP-eF710	Invitrogen	SolA15
KLRG1	PE	BioLegend	2F1/KLRG1
Ly6c	BV650	BioLegend	HK1.4
Ly6c	eF450	Invitrogen	HK1.4
Ly6C	BV421	BioLegend	HK1.4
Ly6G	BV605	BioLegend	1A8
Ly6G	BV785	BioLegend	1A8
Ly6G	PE-Cy5	BioLegend	1A8
MHCII	BV510	BioLegend	M5/114.15.2
MHCII	APC-Fire750	BioLegend	M5/114.15.2
MHCII	BV605	BD Biosciences	M5/114.15.2
MHCII	APC-Cy7	BioLegend	M5.144.15.2
MHCII	PE	Invitrogen	M5/114.15.2
PD-1	BV711	BioLegend	29F.1A12
Thy1.2	AF700	BioLegend	53-2.1
TNF-α	BV650	BioLegend	MP6-XT22
XCR1	BV421	BioLegend	ZET
XCR1	PE	BioLegend	ZET

Supplementary Figures

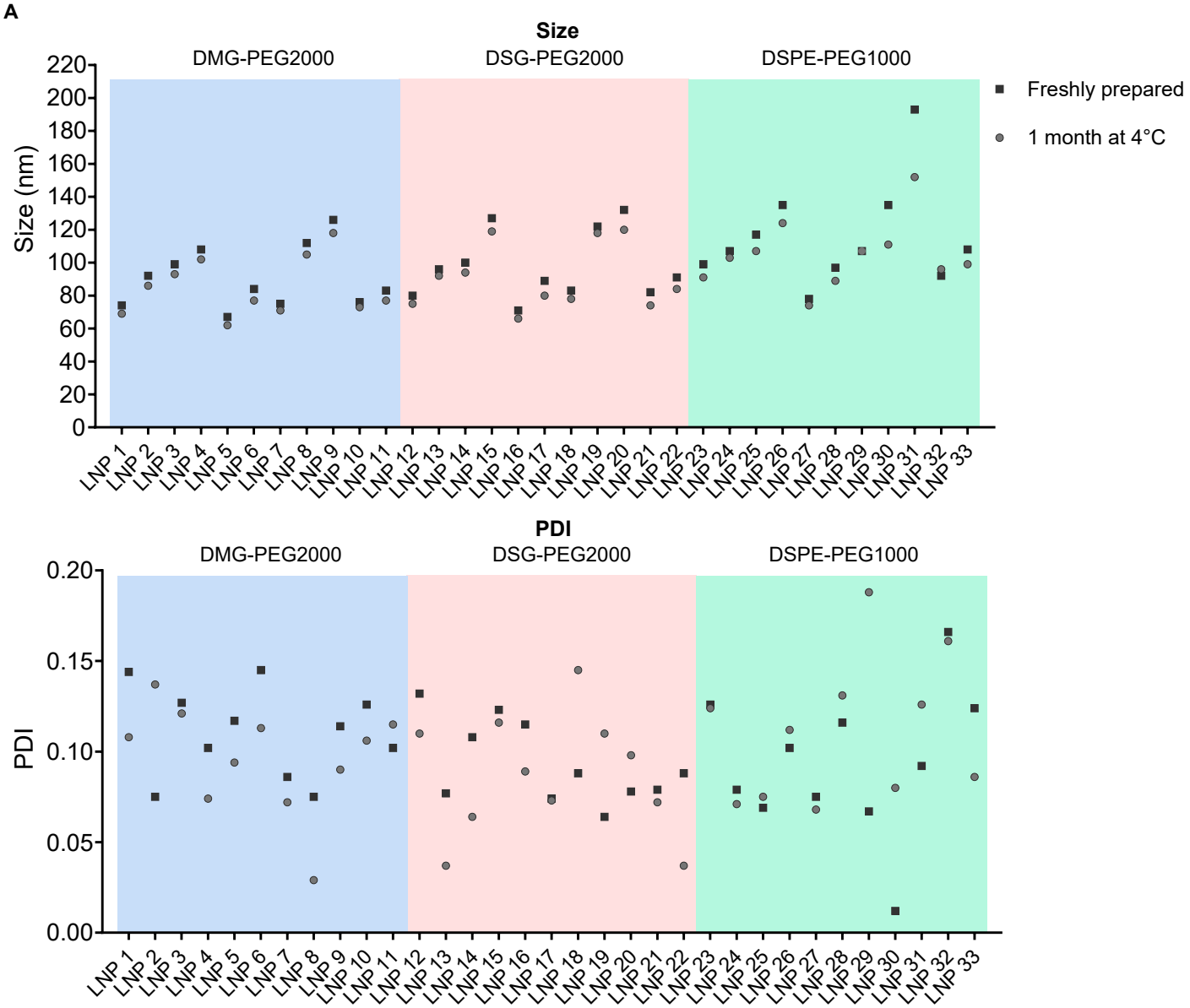

Figure S1. Size and polydispersity index of LNPs remains stable during storage at 4°C.
A) Size and PDI of E7 LNPs used in DOE experiment. B) Size and PDI of E7 LNPs used for validation of the model.
For all LNPs tested, size of LNPs after storage at 4°C (grey circles) does not deviate more than 10% of the size of freshly prepared LNPs (black squares) except for LNP30 and LNP31 which decreased in size by 18% and 21% respectively. PDI remained low (<0.2) during storage at 4°C for all LNPs tested.
Blue background: DMG-PEG2000 LNPs, pink background: DSG-PEG2000 LNPs, green background: DSPE-PEG1000 LNPs

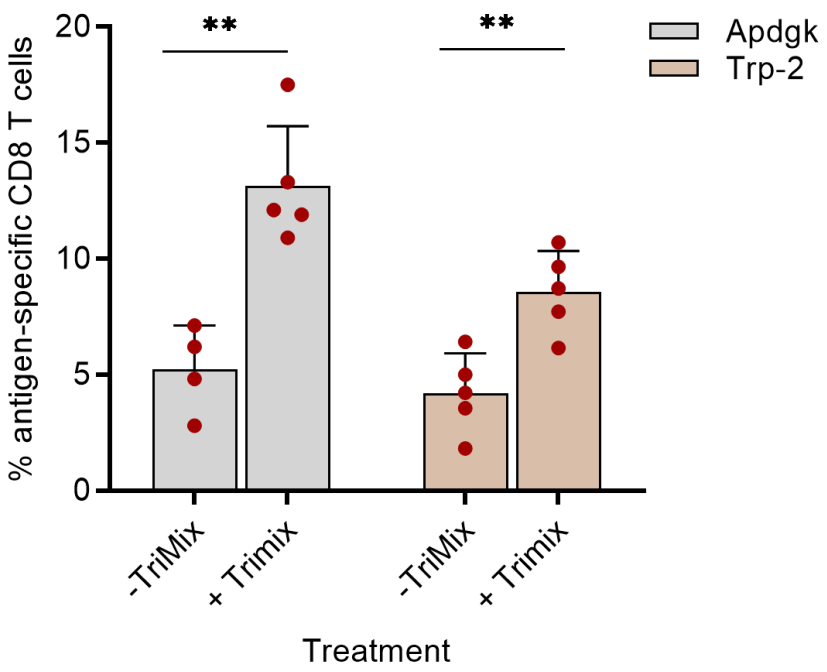

Figure S2. Strong T cell responses are achieved after two immunizations with LNP36 encapsulating mRNA encoding Apdgk or Trp-2 in combination with TriMix.
Mice were injected intravenously two times with weekly interval with 10 µg of mRNA encapsulated in LNP36. mRNA comprised either antigen-encoding mRNA (- Trimix) or a 1:1 mixture of antigen-encoding and TriMix (+ TriMix). Percentages of antigen-specific CD8 T cells in blood were assessed 5 days after the second administration. Data is presented as mean ± SD with individual data points in red, n=4-5. Statistical differences were assessed using two-way Student's t test. **: $p<0.01$.

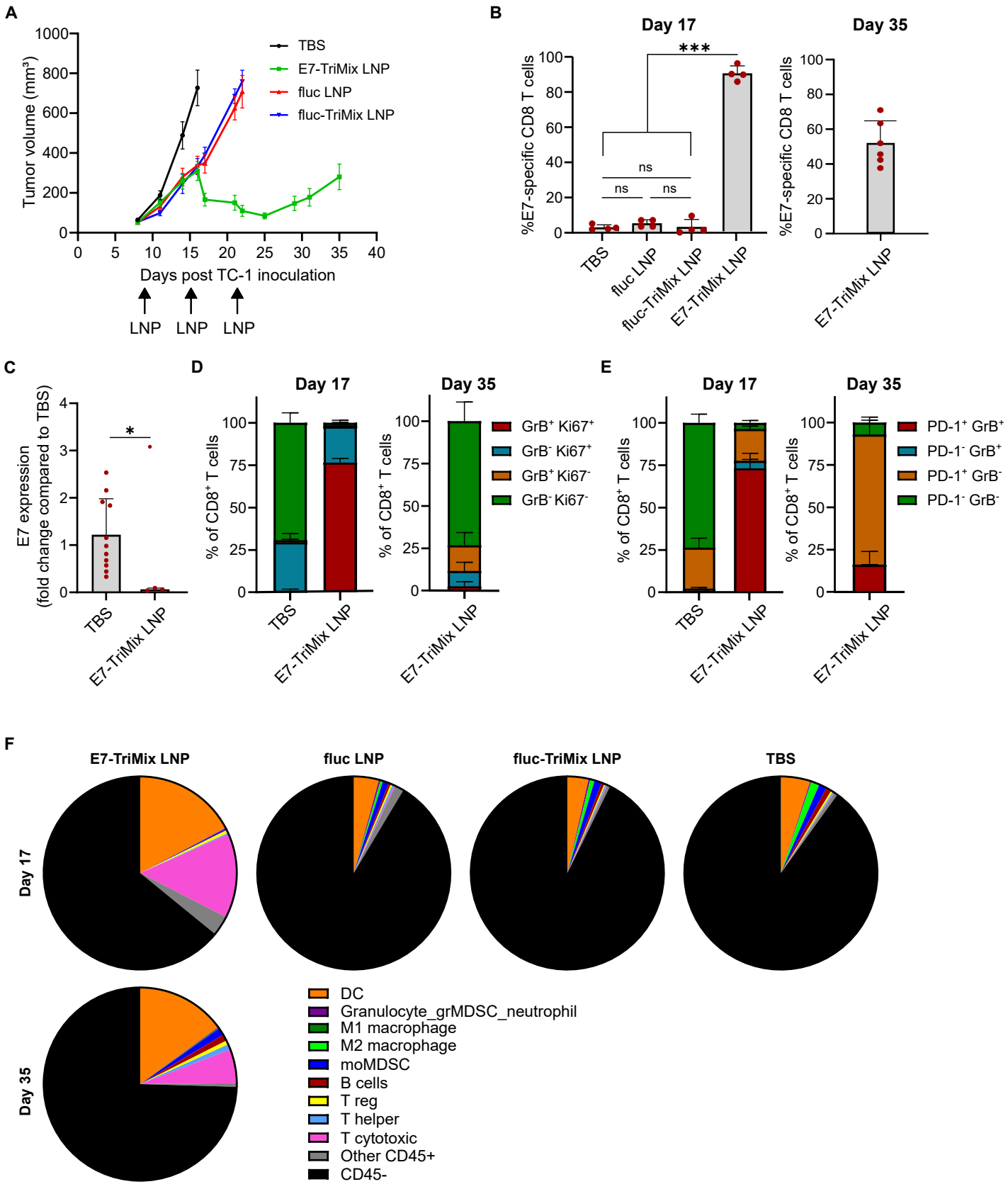
A
Tumor volume (mm³)
Days post TC-1 inoculation
LNP LNP LNP
TBS
E7-TriMix LNP
fluc LNP
fluc-TriMix LNP
B
Day 17
Day 35
%E7-specific CD8 T cells
***
ns
ns
ns
TBS
fluc LNP
fluc-TriMix LNP
E7-TriMix LNP
C
E7 expression
(fold change compared to TBS)
*
D
Day 17
Day 35
% of CD8⁺ T cells
GrB⁺ Ki67⁺
GrB⁻ Ki67⁺
GrB⁺ Ki67⁻
GrB⁻ Ki67⁻
E
PD-1⁺ GrB⁺
PD-1⁻ GrB⁺
PD-1⁺ GrB⁻
PD-1⁻ GrB⁻
F
E7-TriMix LNP
fluc LNP
fluc-TriMix LNP
TBS
Day 17
Day 35
DC
Granulocyte_grMDSC_neutrophil
M1 macrophage
M2 macrophage
moMDSC
B cells
T reg
T helper
T cytotoxic
Other CD45+
CD45-

Figure S3. TC-1 tumors relapse due to decreased TIL infiltration, T cell exhaustion and reduced E7 antigen expression

Mice were injected 3 times i.v. with 5µg fluc, 5µg E7-TriMix (1:1 ratio) or 5µg fluc-TriMix (1:1 ratio) encapsulated in LNP36 or with TBS at a weekly interval. First injection was given at a mean tumor volume of 55mm³. Tumors were harvested at day 17 (all groups) and day 35 (only E7-TriMix LNP group remaining alive) after TC-1 inoculation. **A**: TC-1 tumor growth curves shown as mean ± SEM (n=12). Despite some initial reduced growth rate induced by aspecific immune activation by fluc LNP or fluc-TriMix LNP administration, only E7-TriMix LNP induced tumor regression. **B**: %E7-specific CD8 T cells of the total tumor infiltrating CD8 T cells shown as mean ± SD with individual data points (n=4-6) shown in red. Only after E7-TriMix LNP vaccination a significant infiltration of E7-specific CD8 T cells was noted, which reduced from day 17 to day 35. Statistical differences were assessed using One-Way ANOVA with Tukey's multiple comparison test. **C**: E7 expression in tumors was assessed by RT-qPCR when they reached maximal size (around 1000mm³) for TBS, fluc LNP and fluc-TriMix groups or at day 35 for E7-TriMix LNP. E7 expression was substantially reduced in day 35 tumors of E7-TriMix treated mice. Mean± SD is shown. Statistical differences were assessed using two-tailed t test. **D, E**: Phenotyping of CD8 T cells in the tumor at day 17 (n=4) and day 35 (n=6). CD8 T cells in tumors of E7-TriMix treated mice are mostly Granzyme B^+ $Ki67^+$ (D) and Granzyme B^+ $PD\text{-}1^+$ (E) at day 17, but have lost proliferative and cytolytic capacity at day 35 (tumor relapse). Mean ± SD is shown. **F**: Characterization of the immune cell infiltrate in the tumor at day 17 (average of 4 tumors per group) and day 35 (average of 6 tumors). At day 17, the percentage of CD8 T cells and DC is significantly increased compared to other groups (no significant differences are present between TBS, fluc LNP and fluc-TriMix LNP treatments). At day 35, percentage of CD8 T cells in the tumor is significantly reduced compared to day 17. Statistical differences were assessed using Two-Way ANOVA with Sidak's multiple comparison test. *: $p<0.05$, ***: $p<0.001$, ns: not significant.

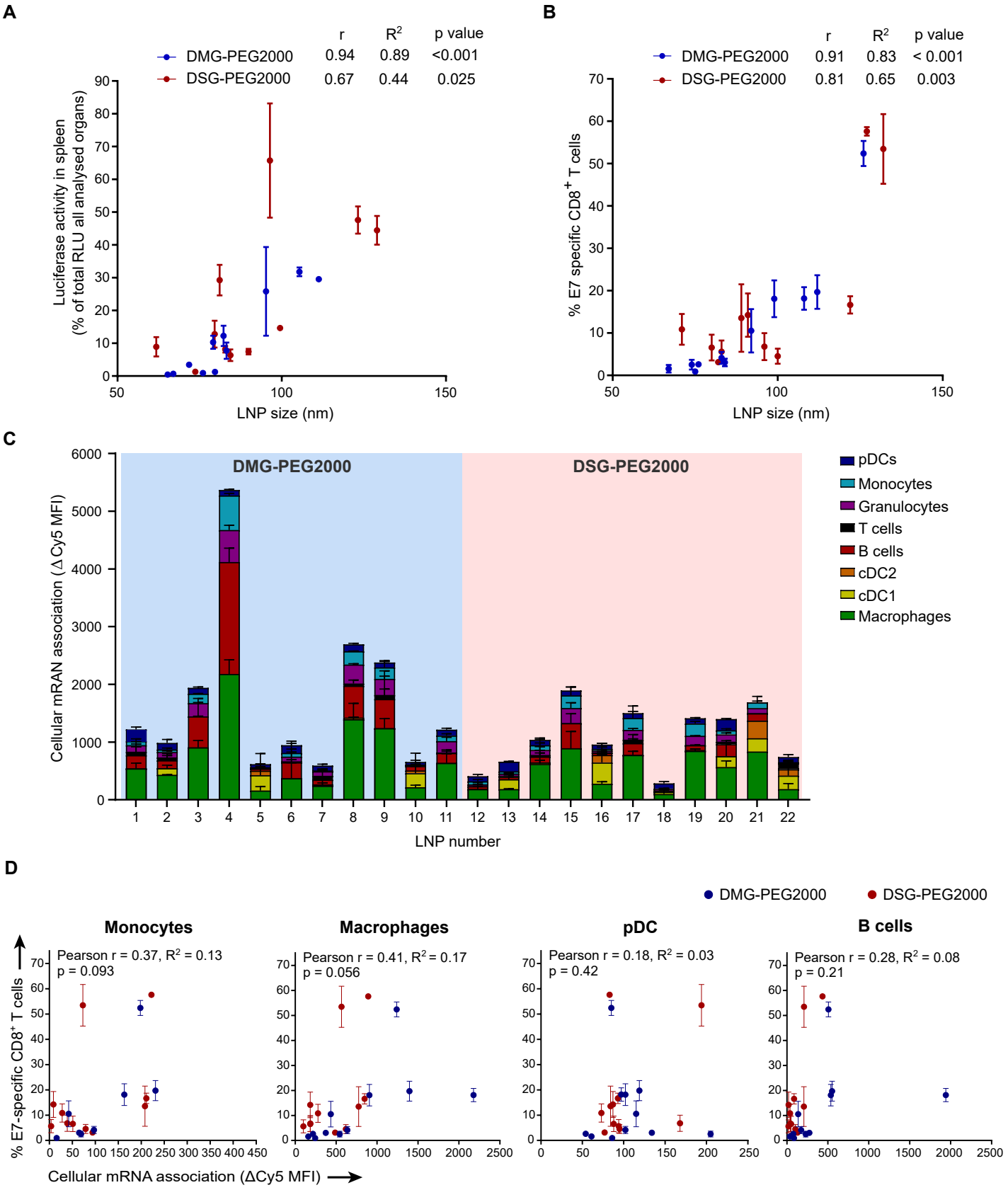
A
r
R²
p value
DMG-PEG2000
0.94
0.89
<0.001
DSG-PEG2000
0.67
0.44
0.025
Luciferase activity in spleen
(% of total RLU all analysed organs)
LNP size (nm)
B
r
R²
p value
DMG-PEG2000
0.91
0.83
< 0.001
DSG-PEG2000
0.81
0.65
0.003
% E7 specific CD8+ T cells
LNP size (nm)
C
DMG-PEG2000
DSG-PEG2000
Cellular mRAN association (ΔCy5 MFI)
LNP number
pDCs
Monocytes
Granulocytes
T cells
B cells
cDC2
cDC1
Macrophages
D
DMG-PEG2000
DSG-PEG2000
Monocytes
Pearson r = 0.37, R² = 0.13
p = 0.093
Macrophages
Pearson r = 0.41, R² = 0.17
p = 0.056
pDC
Pearson r = 0.18, R² = 0.03
p = 0.42
B cells
Pearson r = 0.28, R² = 0.08
p = 0.21
% E7-specific CD8+ T cells
Cellular mRNA association (ΔCy5 MFI)

Figure S4. LNP size and spleen-specific transfection capacity correlate with T cell responses.
A: LNP from the DOE library loaded with Cy5-labeled Fluc mRNA were injected i.v. in mice (n=2-4). After four hours, kidneys, lungs, heart, liver and spleen were isolated, homogenized and assayed for luciferase activity. Luciferase activity in spleen, expressed as percentage of luciferase activity/mg in all assayed organs (Fig. 3C), positively correlated with the size of the injected LNPs based on Pearson correlation coefficients. **B**: E7 mRNA-LNPs were administered intravenously (n=3) three times with a weekly interval. Percentages of E7-specific CD8 T cells in blood after three immunizations (Fig. 1C), as determined by flow cytometry, positively correlated with the size of the injected LNPs, based on Pearson correlation coefficients. **C,D**: Cy5-labeled Fluc mRNA in LNPs was injected i.v. in mice (n=2-4). After four hours, liver non-parenchymal cells were analyzed by flow cytometry to assess Cy5 association with multiple cell types (C). Cellular Cy5 association is expressed as difference between Cy5 mean fluorescence intensity of LNP injected mice and vehicle injected mice (ΔCy5 MFI). In contrast to splenic cell types (Fig. 3E), ΔCy5 MFI of hepatic monocytes, macrophages, pDC and B cells did not correlate with the T cell response after 3 immunizations (D). A,B,C,D: Mean ± SD is shown. RLU=relative light unit. Blue background: DMG-PEG2000-based LNPs, Pink background; DSG-PEG2000-based LNPs.

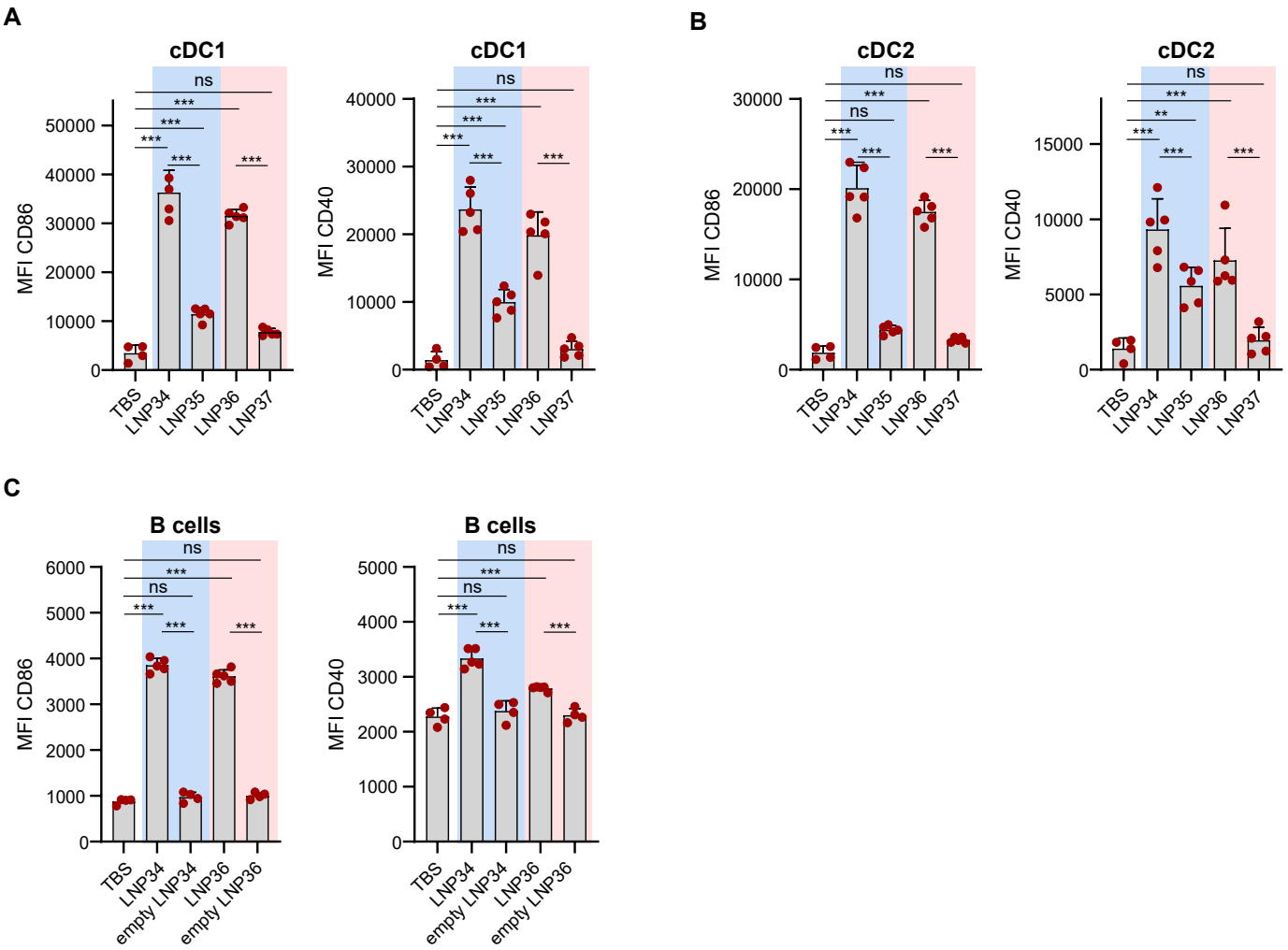

Figure S5. LNP administration induces activation of B cells and DCs.
A,B: E7-TriMix mRNA-LNPs or vehicle controls (TBS) were administered intravenously (n=4-5) and spleens were isolated 4h later for flow cytometry analysis. Geometric Mean Fluorescence Intensity (MFI) of CD86 and splenic cDC1 (A) and cDC2 (B) is strongly upregulated by optimal LNPs (LNP34 and LNP36) and to a lesser extent by non-optimal LNPs (LNP35 and LNP37). **C**: E7-TriMix LNPs or empty LNPs (no mRNA encapsulated) were administered intravenously (n=4-5) and spleens were isolated 4h later for flow cytometry analysis. Geometric Mean Fluorescence Intensity (MFI) of CD86 and CD40 on B cells is significantly upregulated by optimal mRNA-LNPs, but not by optimal empty LNPs. A,B,C: Mean ± SD is shown, with individual data points in red. Statistics were assessed by One-Way ANOVA with Tukey's multiple comparison test. ***: $p<0.001$; ns=not significant. Blue background: DMG-based LNPs, Pink background; DSG-PEG2000-based LNPs.

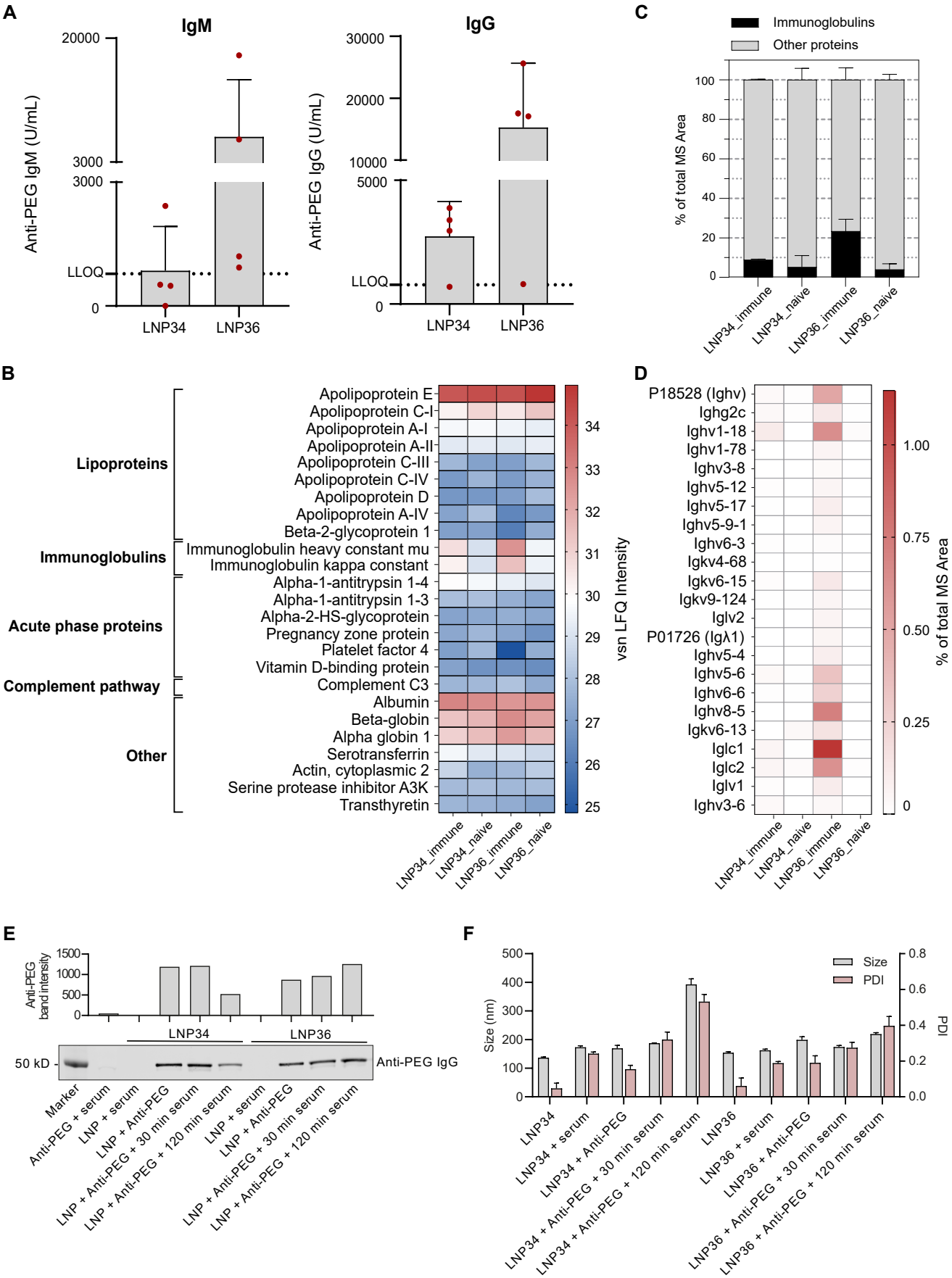
A
IgM
IgG
Anti-PEG IgM (U/mL)
Anti-PEG IgG (U/mL)
20000
3000
LLOQ
0
30000
10000
5000
LNP34
LNP36
B
Lipoproteins
Immunoglobulins
Acute phase proteins
Complement pathway
Other
Apolipoprotein E
Apolipoprotein C-I
Apolipoprotein A-I
Apolipoprotein A-II
Apolipoprotein C-III
Apolipoprotein C-IV
Apolipoprotein D
Apolipoprotein A-IV
Beta-2-glycoprotein 1
Immunoglobulin heavy constant mu
Immunoglobulin kappa constant
Alpha-1-antitrypsin 1-4
Alpha-1-antitrypsin 1-3
Alpha-2-HS-glycoprotein
Pregnancy zone protein
Platelet factor 4
Vitamin D-binding protein
Complement C3
Albumin
Beta-globin
Alpha globin 1
Serotransferrin
Actin, cytoplasmic 2
Serine protease inhibitor A3K
Transthyretin
vsn LFQ Intensity
34
33
32
31
30
29
28
27
26
25
LNP34_immune
LNP34_naive
LNP36_immune
LNP36_naive
C
Immunoglobulins
Other proteins
% of total MS Area
100
80
60
40
20
0
D
P18528 (Ighv)
Ighg2c
Ighv1-18
Ighv1-78
Ighv3-8
Ighv5-12
Ighv5-17
Ighv5-9-1
Ighv6-3
Igkv4-68
Igkv6-15
Igkv9-124
Iglv2
P01726 (Igλ1)
Ighv5-4
Ighv5-6
Ighv6-6
Ighv8-5
Igkv6-13
Iglc1
Iglc2
Iglv1
Ighv3-6
1.00
0.75
0.50
0.25
0
% of total MS Area
E
Anti-PEG band intensity
1500
1000
500
0
LNP34
LNP36
50 kD
Anti-PEG IgG
Marker
Anti-PEG + serum
LNP + serum
LNP + Anti-PEG
LNP + Anti-PEG + 30 min serum
LNP + Anti-PEG + 120 min serum
F
Size
PDI
Size (nm)
500
400
300
200
100
0
0.8
0.6
0.4
0.2
0.0
LNP34
LNP34 + serum
LNP34 + Anti-PEG
LNP34 + Anti-PEG + 30 min serum
LNP34 + Anti-PEG + 120 min serum
LNP36
LNP36 + serum
LNP36 + Anti-PEG
LNP36 + Anti-PEG + 30 min serum
LNP36 + Anti-PEG + 120 min serum

Figure S6. LNPs induce anti-PEG antibodies and show differential interactions with mouse plasma proteins. **A**: Mice were immunized three times with E7 mRNA, encapsulated in LNP34 or LNP36, on days 0, 7 and 14 to induce T cell responses. On day 54 (40 days after the last immunization), serum was collected anti-PEG IgM andIgG titers were analyzed by ELISA. When in a separate experiment mice were boosted with mRNA-LNPs at day 55, high percentages of E7-specific T cells were observed (Fig. 2A). It is therefore unlikely that anti-PEG antibodies interfere with the boostability of the mRNA-LNP vaccines. Mean ± SD is shown, with individual data points in red. LLOQ = lower limit of quantification. **B,C,D**: Mice were immunized twice with a weekly interval with E7-TriMix mRNA encapsulated in LNP34 or LNP36. Blood plasma was collected 6 days after the last immunization. Additionally, plasma from naive (non-immunized) mice was collected. LNPs were incubated with plasma of naive mice or mice immunized with the same LNPs, followed by centrifugation of the complexes, precipitation of proteins, digestion to peptides and analysis by mass spectrometry. Details on method/analysis are included in Supplementary methods. **B**:Identified proteins were sorted by the average LFQ (label-free quantification) intensity values over all samples (LNP34 and LNP36 incubated with immune or naive plasma). Figure shows the 25 proteins with the highest average intensities, grouped by functionality. These proteins consist mainly of common serum proteins (e.g. albumin), lipoproteins, immunoglobulins, acute phase proteins and complement. Mean of replicates (n=3) is used to construct heatmap. **C**: The percentage of the total MS area (sum of LFQ intensity values of all identified proteins) classified as immunoglobulins is clearly increased in samples obtained from incubation of LNP36 with immune plasma compared to naive plasma. Mean ± SD is shown. **D**: The percentage of the total MS area of the differentially enriched (DE) immunoglobulins in LNP34 (only Ighv3-6) and LNP36 samples. DE proteins H1-2 and Gm8797, which are reduced in intensity in LNP36 immune plasma compared to naive plasma (Fig. 5F), are excluded from the heatmap. Several immunoglobulins are clearly more abundant in samples obtained from incubation of LNP36 with the respective immune plasma than from LNP34 incubation. Median of replicates (n=3) is used for heatmap. **E**: Western blot and band intensity quantification of LNPs incubated with anti-PEG antibodies and/or mouse serum and subjected to size-exclusion chromatography to remove free antibodies. In control lane 'anti-PEG + serum', typical LNP-containing fractions of a serum/antibody sample without LNPs was loaded to show the capacity of the column to separate LNPs from free anti-PEG. Anti-PEG opsonization of LNP34, but not of LNP36, is reduced after 2h incubation with serum. **F:** Size and polydispersity index (PDI) of LNPs after incubation in serum and/or anti-PEG antibodies. Size of LNP34, but not of LNP36, is increased after 2h incubation with serum and antibodies. Mean ± SD of 3 replicate measurements is shown.

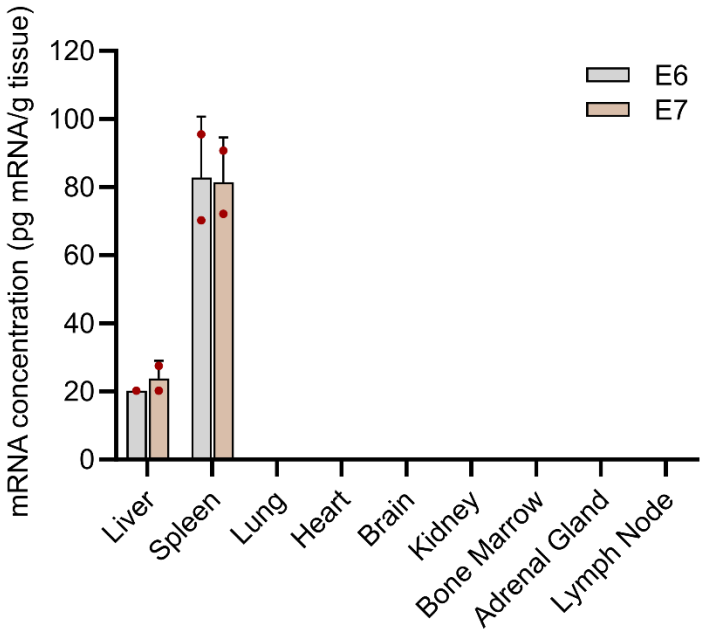

Figure S7. mRNA-LNPs distribute mainly to spleen in non-human primates at lower doses.
After 2 intravenous immunizations with 40µg of mRNA (formulated as a mixture of LNP36 containing either E6 or E7 mRNA and TriMix), mRNA strongly accumulated in spleen of non-human primates, similar to when a 100µg dose was administered (Fig. 5G). Mean ± SD is shown, with individual data points in red (n=2).

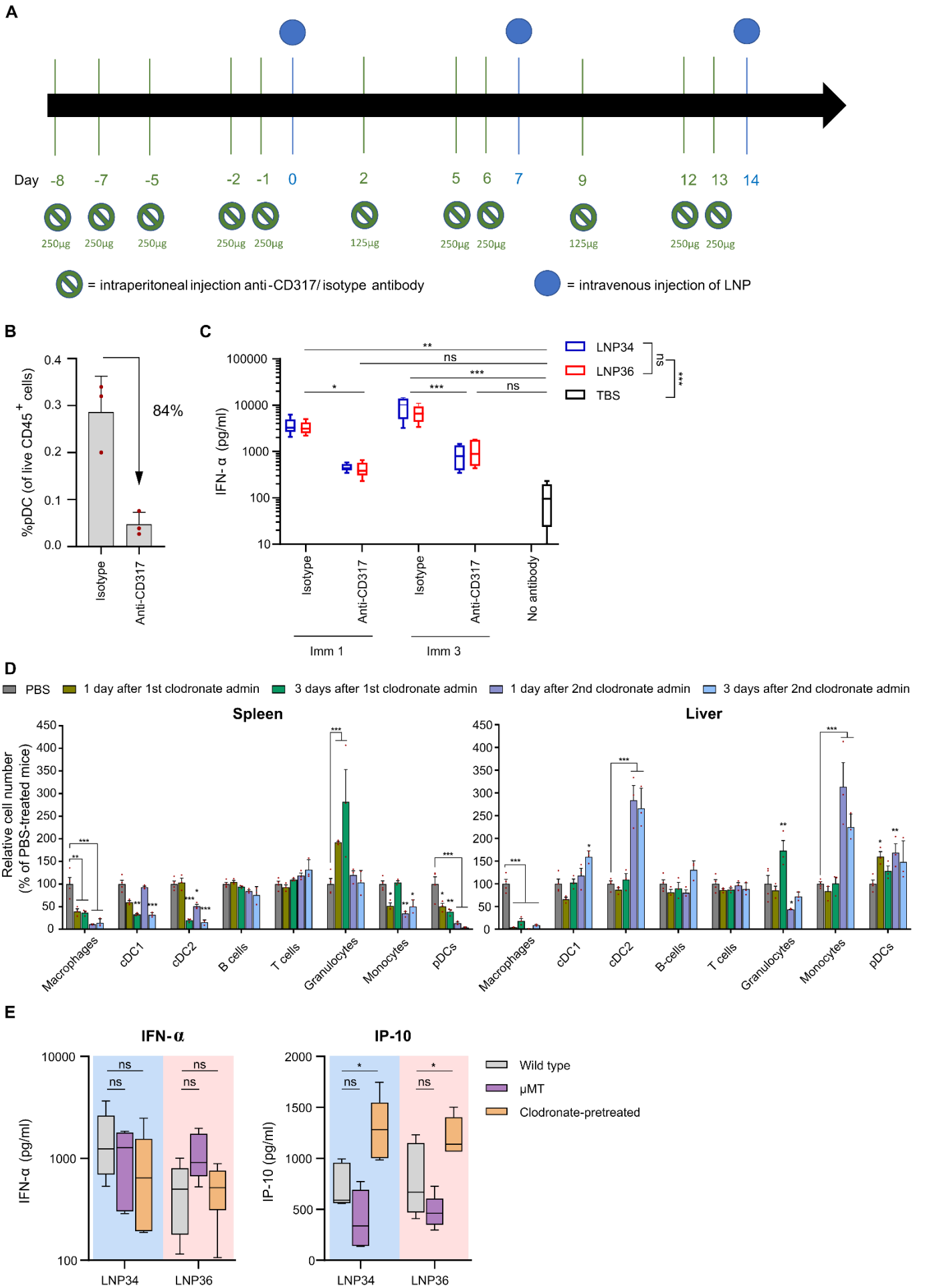
A
Day -8 -7 -5 -2 -1 0 2 5 6 7 9 12 13 14
250µg 250µg 250µg 250µg 250µg 125µg 250µg 250µg 125µg 250µg 250µg
= intraperitoneal injection anti-CD317/ isotype antibody
= intravenous injection of LNP
B
%pDC (of live CD45+ cells)
84%
Isotype
Anti-CD317
C
IFN-α (pg/ml)
LNP34
LNP36
TBS
ns
***
Isotype
Anti-CD317
Isotype
Anti-CD317
No antibody
Imm 1
Imm 3
D
PBS
1 day after 1st clodronate admin
3 days after 1st clodronate admin
1 day after 2nd clodronate admin
3 days after 2nd clodronate admin
Spleen
Liver
Relative cell number (% of PBS-treated mice)
Macrophages
cDC1
cDC2
B cells
T cells
Granulocytes
Monocytes
pDCs
B-cells
E
IFN-α
IP-10
IFN-α (pg/ml)
IP-10 (pg/ml)
LNP34
LNP36
Wild type
µMT
Clodronate-pretreated

Figure S8. Validation of pDC and phagocyte depletion models.
A: Treatment regimen used for depleting pDCs, by intraperitoneal injection of anti-CD317 or isotype control antibody. **B**: Six control mice were included in the experiment to confirm successful pDC depletion. At typical days of LNP immunization (day 0, 7 and 14), spleens of the control mice injected with isotype or anti-CD317 (scheme in A) were isolated and the percentage of pDCs was analyzed using flow cytometry. pDC percentage within the live CD45+ cell population was on average (at all three timepoints) 84% lower in anti-CD317-treated mice compared to isotype-treated mice. **C**: IFN-α levels after immunization with E7-TriMix-loaded LNPs were significantly reduced in pDC depleted mice compared to isotype control antibody injected mice, but remained elevated (not significant) compared to TBS buffer injected mice, indicating there are also other cell types than pDC producing IFN-α. Statistical differences were assessed by Two-Way ANOVA with Tukey's multiple comparison test **D**: Depletion of phagocytes in spleen and liver after intravenous injection of clodronate liposomes was assessed by flow cytometry 1 and 3 days after first and second administration (1 week interval) of clodronate liposomes. Macrophages were significantly depleted in both organs at all assessed timepoints, but also reduced numbers of DCs and monocytes were observed in spleen. Statistical differences were assessed by One-Way ANOVA with Dunnett's multiple comparison test. **E**: IFN-α cytokine levels were not significantly different in μMT and clodronate-treated mice compared to wild type mice after LNP immunization. IP-10 was slightly increased in clodronate-treated mice, but similar in μMT mice, compared to wild type mice, as determined by One-Way ANOVA with Dunnett's multiple comparison test. *: $p<0.05$, **: $p<0.01$, ***: $p<0.001$, ns: not significant.